Boundary-Layer Meteorology (2023) 189:5–52
https://doi.org/10.1007/s10546-023-00821-1

RESEARCH ARTICLE

Understanding Thermally Driven Slope Winds: Recent Advances and Open Questions

Sofia Farina[1,2] · **Dino Zardi**[1,2]

Received: 12 February 2022 / Accepted: 3 July 2023 / Published online: 9 September 2023

Abstract
The paper reviews recent advances in our understanding about the dynamics of thermally driven winds over sloping terrain. Major progress from recent experiments, both in the field and in the laboratory, are outlined. Achievements from numerical modelling efforts, including both parameterized turbulence and large eddy simulation approaches, up to direct numerical simulations, are also reviewed. Finally, theoretical insights on the nature of turbulence in such winds are analyzed along with applications which benefit from progress in understanding of these flows. Open questions to be faced for further investigations are finally highlighted.

Keywords Anabatic wind · Boundary-layer meteorology · Katabatic wind · Slope · Turbulence

1 Introduction

Atmospheric dynamics near the Earth's surface are strongly affected by heat fluxes, which are mostly modulated either by the diurnal cycle of daytime incoming solar radiation and nighttime radiative loss, or by persistent cooling during long nights in the polar regions. In particular, over non-horizontal terrain, the warming/cooling of air adjacent to the surface promotes buoyancy-driven upslope/downslope winds. Their dynamics, including remarkable turbulence effects, have been extensively explored, under various situations, by means of many experiments, either in the field or in the laboratory. More recently, extensive high-resolution numerical model simulations have greatly expanded our capability of investigating these airflows.

Thermally driven winds are closely tied to specific topographic features of each mountain area. Hence, they contribute to characterize its (micro-)climate. Despite their relevance, they are still poorly represented in operational numerical weather prediction models (Chow et al. 2019; De Wekker et al. 2018; Emeis et al. 2018; Serafin et al. 2018). One reason is the limited resolution allowed by the available computational resources for operational purposes.

✉ Sofia Farina
s.farina@unitn.it

[1] Atmospheric Physics Group, Department of Civil, Environmental and Mechanical Engineering, Trento, Italy

[2] Center for Agriculture Food Environment (C3A), University of Trento, Trento, Italy

Another reason is the inadequate representation of the surface-atmosphere exchanges in their parameterizations (Jiang and Doyle 2008; Barthélemy et al. 2012; Poulos and Zhong 2008; Chow et al. 2019). Accordingly, the need for more accurate representations of orographic factors stimulated various research efforts, including targeted field experiments and extensive modelling exercises.

The chapter on daily periodic mountain wind system by Zardi and Whiteman (2013) includes a section on slope winds, reviewing the state of the art on the topic up to 2012. The present paper builds on it, summarizing advances achieved in the last two decades.

This article is structured as follows: Sect. 2 reviews observations from field campaigns and laboratory experiences; Sect. 3 outlines advances from numerical simulations, arranged in subsections according to the techniques adopted; Sect. 4 describes the main advances in the analytical description of slope winds; Sect. 5 is focused on stability and oscillations and finally, Sect. 6 recalls paradigmatic cases and particular applications.

2 Outcomes from Experiments

2.1 Major Field Campaigns

Various field campaigns were carried out in the last two decades, as part of research projects investigating atmospheric processes over complex terrain. Tables 1 and 2 provide a comprehensive overview of them. Most of these observational efforts allowed also investigating slope winds, and their connections with ambient conditions, and other concurring atmospheric flows. Here we briefly recall the concepts, locations and instrumental layouts of these experiments.

MAP-Riviera project within the Mesoscale Alpine Programme MAP (1999)

The MAP-Riviera project analysed boundary layer (BL) processes developing in the U-shaped Riviera Valley (Swiss Alps), including turbulent exchanges of heat, moisture and momentum on a sidewall slope and their connections with valley winds (Rotach et al. 2004). The valley is approximately 15 km-long and 1.5 km-wide. The floor is at 250 m ASL and

Table 1 Field campaigns including measurements of slope winds performed over the last two decades

Years	Experiment	Site	References
1999	MAP	Riviera Valley (Switzerland)	Rotach et al. (2004)
2006	METCRAX	Meteor Crater (USA)	Whiteman et al. (2008)
2006	TRANSFEX	Phoenix (USA)	Fernando et al. (2013)
2010	SELF-2010	Ferret Valley (Switzerland)	Nadeau et al. (2013)
2011	BLLAST	Plateau de Lannemezan (France)	Lothon et al. (2014)
2012	MATERHORN	Granite Mountain (USA)	Fernando et al. (2015)
2013	METCRAX II	Meteor Crater (USA)	Lehner et al. (2015)
2016	–	Okanagan Valley (Canada)	Everard et al. (2020)
2018	PERDIGAO	Vale Cobrao (Portugal)	Fernando et al. (2019)
2011–25	I-BOX	Inn Valley (Austria)	Rotach et al. (2017)
2019	–	Belledonne (France)	Charrondière et al. (2020)
2023–24	TEAMx	Inn and Adige Valleys (Italy, Austria)	Serafin et al. (2020)

Table 2 Field campaigns including measurements of katabatic winds over glaciers performed over the last two decades

Years	Site	References
1996	Pasterze Glacier (Austria)	Denby and Smeets (2000)
1996	Vatnajokull Ice Cap (Iceland)	Denby and Smeets (2000)
1996	Breidamekurjokull Glacier (Iceland)	Parmhed et al. (2004)
1998	Morteratschglescher (Switzerland)	Oerlemans and Grisogono (2002)
1998	West Greenland Ice Sheet (Greenland)	Oerlemans and Grisogono (2002)
2010	Castle Creek Glacier (Canada)	Radić et al. (2017)
2015–16	Dumont d'Urville (Antartica)	Grazioli et al. (2017)

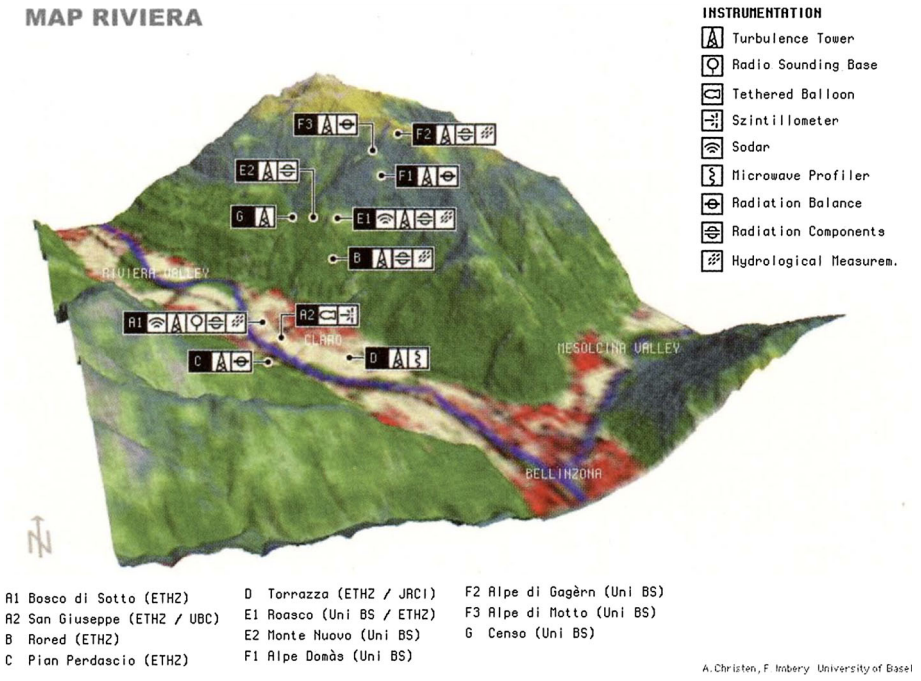

Fig. 1 Topography and land use of the Riviera Valley, and instrumental layout of the MAP-Riviera campaign (reproduced with permission from Rotach et al. (2004))

sidewall ridge-tops at about 2500 m ASL, with slope angles 30° on the Eastern sidewall and 35° on the Western. Measurements were taken at 11 sites (Fig. 1) from 10 July to 13 October 1999. Turbulence measurements were taken at 9 towers, one on the valley floor, all the others on the eastern slope (covering both forests and meadows).

Meteor Crater Experiments METCRAX-I and METCRAX-II

The experiments focused on cold air pools, and their connections with thermally driven circulations. Measurements were performed in the Meteor Crater in Northern Arizona (USA), a near-circular crater approximately 165 m deep and 1.2 km wide at the rim, for the entire month of October 2006 (Whiteman et al. 2008). The experiment deployed a variety of ground

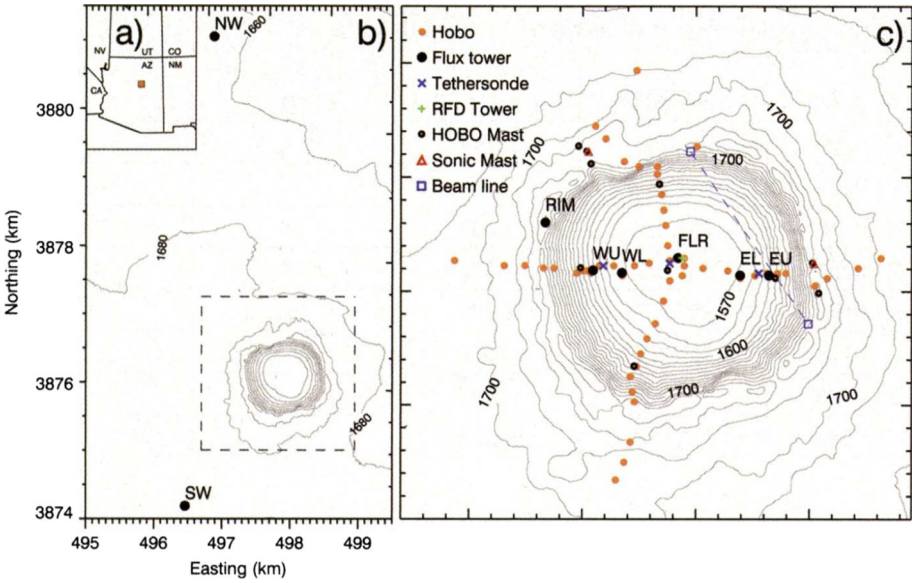

Fig. 2 Map of the area and instrumentation of the first METCRAX campaign, in the Arizona Meteor Crater (reproduced with permission from Whiteman et al. 2008)

based instrument, including six towers equipped for turbulence measurements, mostly at sites with steep slopes. METCRAX-II explored downslope windstorms-type flows and their controlling parameters, in the same target area of METCRAX-I, for the entire month of October 2013 (Lehner et al. 2016). Instruments were installed both upstream of the crater, to observe wind and temperature profiles, and within the crater, to monitor the flow response to ambient conditions.

Slope Experiment near La Fouly SELF-2010 (2010)

SELF-2010 investigated the surface-atmosphere interplay during the evening transition from radiation budgets and atmospheric profiles on a west-facing slope in the narrow 12-km-long Val Ferret in the Swiss Alps (Fig. 3), in July-September 2010 (Nadeau et al. 2013). Instruments were deployed along the slope and included a single-level turbulence and radiation tower, a multi-level 10 m turbulence tower, two wireless weather stations, and five thermal infrared sensing stations.

Mountain Terrain Atmospheric Modeling and Observations MATERHORN (2013)

MATERHORN aimed at improving short-range forecasting of near surface variables by means of new turbulence closures and BL parameterizations. Measurements were taken at the Granite Mountain Atmospheric Science Testbed, 137 km southwest of Salt Lake City (Utah), a wide area (3700 km^2) of desert shrub and playa in complex terrain surrounding Granite Mountain, a 11.8-km-long and 6.1-km-wide massif (Fig. 4). The campaign was performed during two 35-day sub-campaigns, in fall 2012 and spring 2013 (Fernando et al. 2015). Six intensive observation sites (IOS), including a whole slope, were densely equipped with instrumentation (Fig. 4).

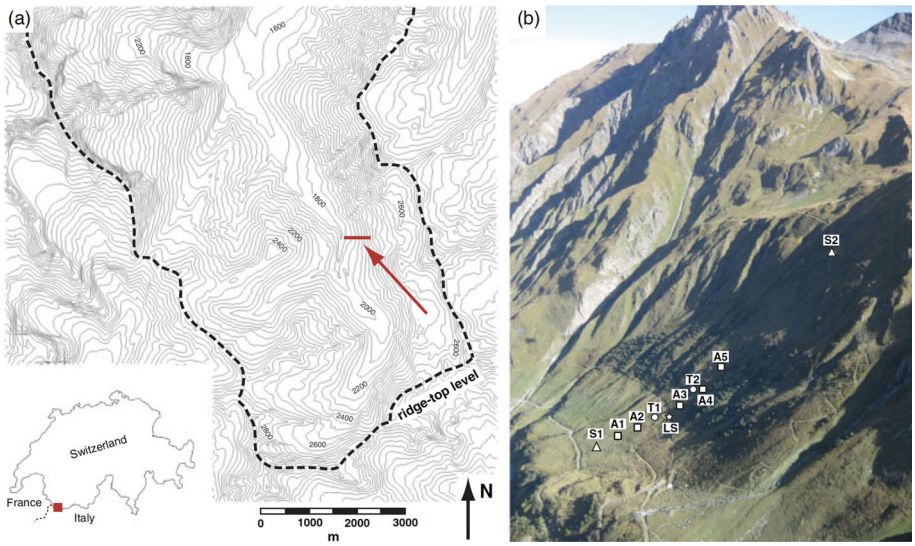

Fig. 3 **a** Map of Val Ferret (contour levels every 50 m) and **b** view of the experimental site of SELF-2010 campaign (Reproduced with permission from Nadeau et al. 2013)

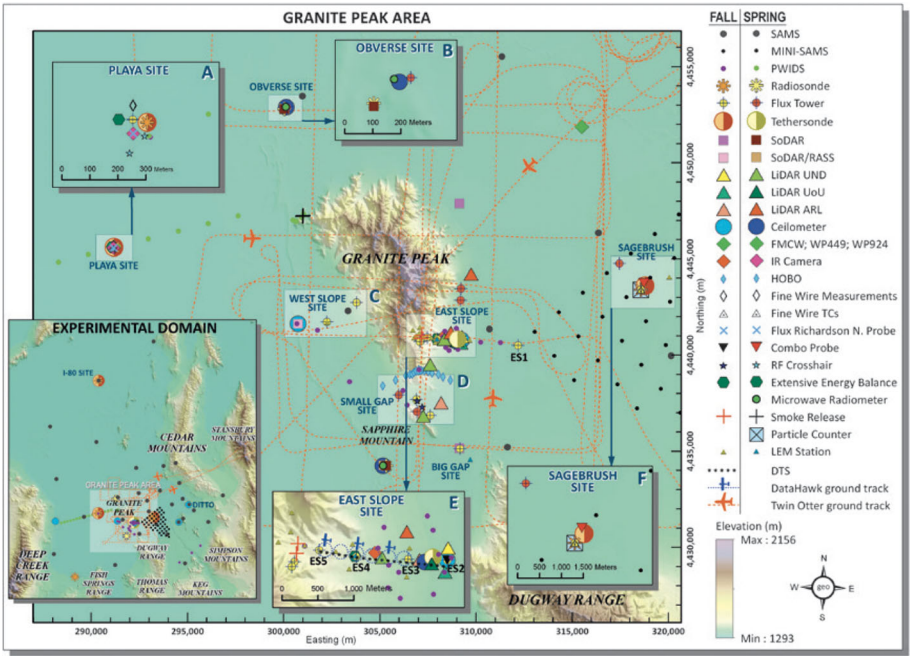

Fig. 4 Measurement sites of MATERHORN in Salt Lake Desert (Utah) and overview of their equipment (Reproduced with permission from Fernando et al. 2015)

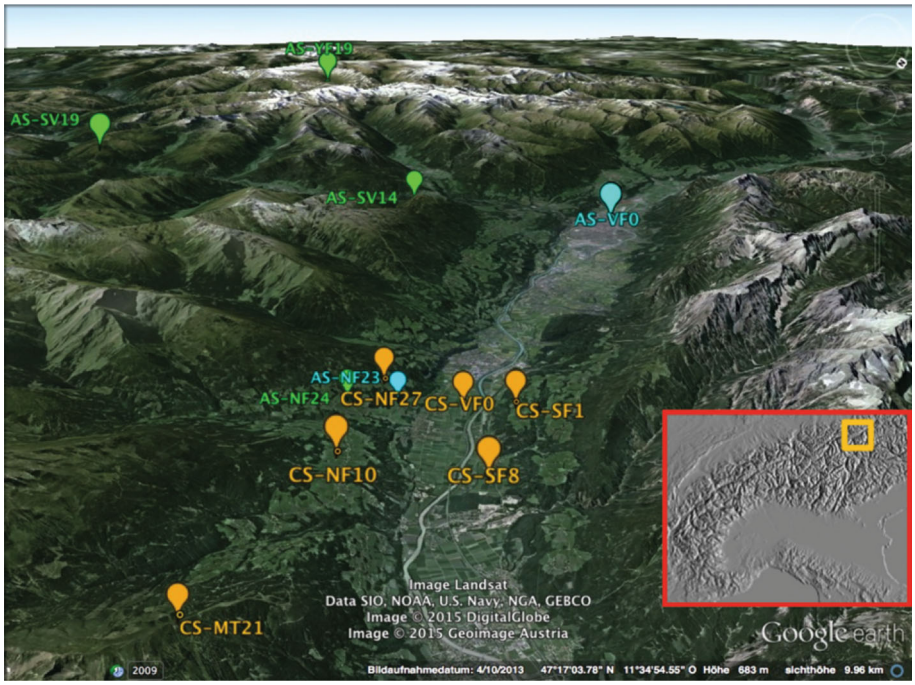

Fig. 5 Map of the I-BOX target area, including instrumented sites (reproduced with permission from Rotach et al. 2017)

Innsbruck I-box (2011–2025)

The ongoing I-box project aims at monitoring the spatial variability of turbulence in the Inn Valley (Austria) and investigating connections with local and mesoscale flows. The Inn valley is a major U-shaped valley with a floor width of 2–3 km and a ridge-to-ridge distance less than 20 km (Rotach et al. 2017). The campaign was planned to operate from 2011 to 2025. The setup includes several measurement sites (Fig. 5), and representative of different situations (valley floor, south-facing and north-facing sidewalls, mountain tops). Each site includes a tower equipped with 2 to 4 turbulence measurement levels.

High-altitude steep slope in Belledonne Mountain (France)—2012 and 2019

Two campaigns (14–23 November 2012 and 12–28 February 2019, with snow-covered surface) investigated katabatic winds over a steep slope in Belledonne Mountain near Grenoble in the French Alps (Charrondière et al. 2020, 2022). A 7 m-mast was equipped with instruments for turbulence measurements at different levels down to very close to the surface (Fig. 6).

Measurements over sloped vineyards in Southern Okanagan Valley (2016)

This experiment explored the interplay between turbulence in slope flows and a trellised vineyard on a 7° slope in the Southern Okanagan Valley (British Columbia, Canada) during three weeks in July 2016 (Everard et al. 2020). A single tower equipped with five measurement levels was used, each equipped with ultrasonic anemometers and fine-wire thermocouples.

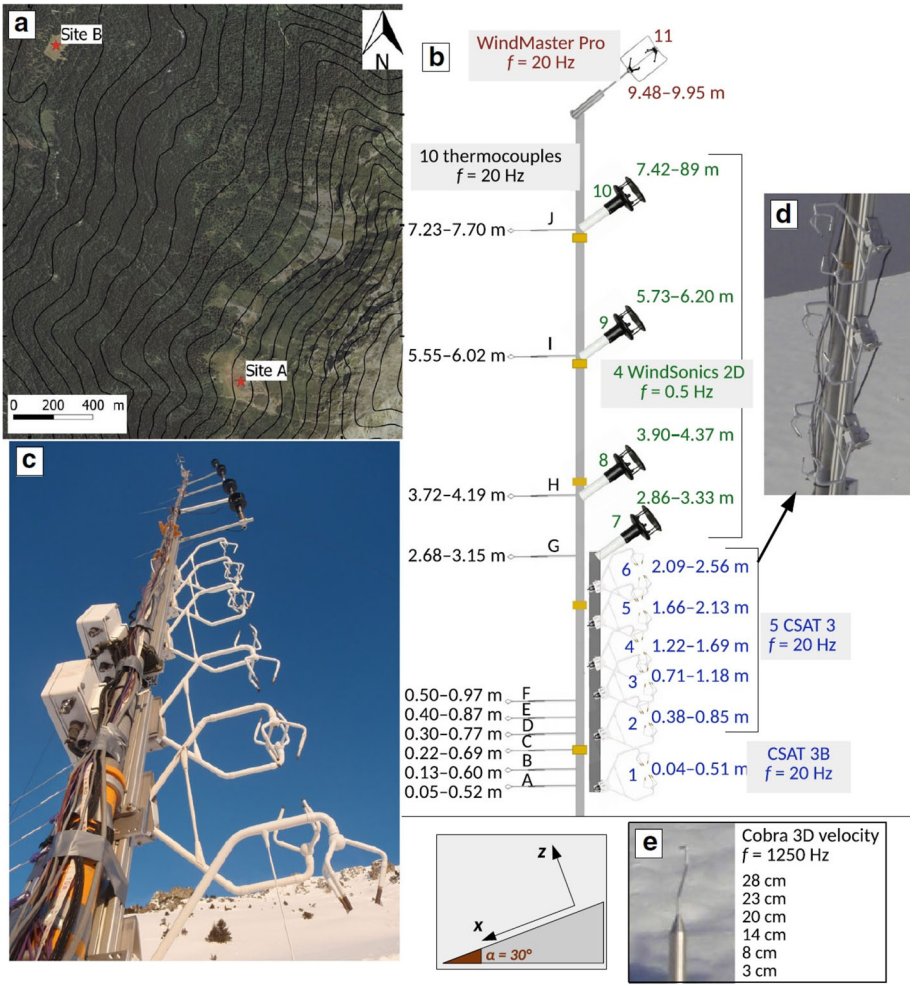

Fig. 6 **a** Map of measurements sites A and B on Belledonne Mountain. **b** Layout of the mast and heights of turbulence sensors (f is the sampling frequency). **c** View of the mast. **d** Fixing system of the CSAT sensors. **e** Cobra pitot-type probe and heights where it was operated (reproduced with permission from Charrondière et al. 2022)

Perdigao (2017)

The Perdigao field campaign was designed to create a comprehensive high-resolution dataset to fill knowledge gaps in wind-energy physics. The experiment goals included developing new parameterizations in numerical weather prediction models and providing a reliable benchmark for their validation. Measurements were performed between 1 and 15 May 2017 in Vale de Cobrao (Portugal). The topography of the valley exhibits an almost idealized shape of a two-dimensional valley within parallel ridges. The core instrumental equipment consisted in 49 towers with 195 sonic anemometers, accompanied by scanning and profiling lidars, a radio acoustic sounding system, a sodar, a radiosonde, microwave radiometers, tethered balloons, a scintillometer, a ceilometer, acoustic sensors, seismometers, high-resolution microbarometers, and an aerosol particle-sizing instrument (Fernando et al. 2019).

2.2 Major Achievements from Field Measurements

2.2.1 Criteria for the Identification of Slope Wind Days

The ideal conditions conducive to the full development of pure thermally-driven winds are typically associated with clear skies and absent or weak upper winds. However such ideal unperturbed situations need to be objectively defined in terms of observable quantities. A significant part of the recent literature concentrated on quantifying the conditions controlling the onset of either up- or downslope winds. This goal turned out to be more challenging for upslope than for downslope winds. The latter are usually associated with strong stability, hence constrained to follow quite closely the local topography. Instead, thermal convection, which is inherently associated with upslope winds, may react quite diversely over different landforms. Also, upslope layers are more prone to convection which, may promote separation of thermals from the surface, especially under weak ambient stability. Hence the flow patterns may only loosely follow the terrain shape. Moreover, the surface energy budget (SEB) under nocturnal cooling is usually dominated by surface processes and less exposed to upper unpredictable factors, whereas solar radiation feeding upslope winds may be significantly reduced, even by intermittent and randomly scattered cloud shading.

Hence various criteria were proposed in the literature, to identify conditions favouring the development of valley winds (Giovannini et al. 2017; Lehner et al. 2019), or, generally, thermally driven circulations (Román-Cascón et al. 2019). Most of them include requirements on synoptic wind speed, thermal structure of the free troposphere, atmospheric pressure gradients, and radiation. In particular, Arrillaga et al. (2018) adapted a method, originally devised for sea-breeze events, and outlined a method consisting in four requirements: (i) weak large-scale winds, (ii) absence of synoptic cold fronts, (iii) no precipitation, and (iv) persistence of the wind in the katabatic direction for a minimum duration. A different criterion, specifically meant for katabatic flows, was adopted by Stiperski et al. (2020) and Charrondière et al. (2020, 2022), and consists in three conditions: (i) wind direction steadily downslope, (ii) slope-normal wind profiles consistent with a jet-like structure, and (iii) a positive vertical temperature gradients.

More recently, ? proposed a complementary criterion specifically meant for identifying conditions favourable to anabatic winds. The criterion is based on average daily radiation, air pressure, and overall synoptic conditions, without any *a priori* prescription on wind direction.

2.2.2 Basic Thermal and Dynamical Structure

Katabatic winds

The basic mechanisms underlying katabatic flows are quite intuitively explained in terms of surface radiative cooling, producing colder and denser air flowing downslope under the effect of gravity (Whiteman 2000). However, field observations and numerical simulations outlined subtle and nontrivial features, characterising different kinds of katabatic flows.

Earlier observations of katabatic flows in mountain valleys allowed identifying their main features (schematically summarised in Fig. 7): (i) they develop early after sunset, following surface cooling, (ii) they develop under clear skies and quiescent synoptic conditions, (iii) their depth may range from few tens to a few hundred meters, (iv) they form within a developing temperature inversion, (v) the wind speed increases from the ground up to to 2–6 ms^{-1} and then decreases again from this jet to the top of the inversion (Banta et al. 2004; Darby et al. 2006; Poulos and Zhong 2008; Zhong and Whiteman 2008; Stiperski

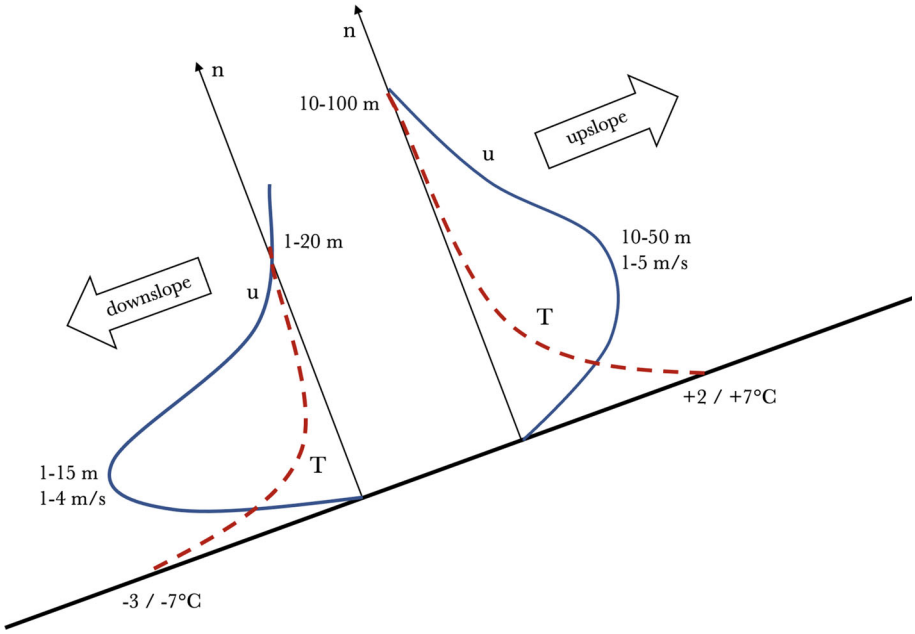

Fig. 7 Schematic representation of the main differences between the features of katabatic and anabatic flows as observed from experimental data. The main features reported are the height and the intensity of the jet and the strength and height of the temperature inversion (adapted from Whiteman 2000)

et al. 2007; Princevac and Fernando 2007; Savage III et al. 2008; Jiang and Doyle 2008; Heinemann 2002; Arrillaga et al. 2018; Cuxart et al. 2020; Charrondière et al. 2020). With strongly stratified ambient atmospheres and steep slopes, the main features defining the flow, in particular wind strength and layer depth, do not vary significantly with downslope distance (Haiden and Whiteman 2005; Whiteman and Zhong 2008). Hence usually a one-dimensional approximation is adopted, and all quantities are considered depending only on the height above ground. However, oscillations in the direction of the flow have been observed, which brought to call for a two-dimensional structure of the flow, and to question the homogeneity in the cross-slope direction (Haiden and Whiteman 2005). Their causes can be identified in weak large-scale pressure perturbations. Including such oscillations in model simulations determined significant changes in the position of the katabatic jet (Oldroyd et al. 2014).

Over gentle slopes in mid-latitudes, katabatic flows are generally quite weak, and their jet peaks are found at heights z_{jet} ranging from a few to several tens of meters above ground. Hence they are sometimes categorised as *deep* katabatic flows (Stiperski et al. 2020). On the contrary, in polar regions and over glaciers, or over steeper slopes even in mid-latitudes, shallower and stronger flows are usually observed, exhibiting jets very close to the ground (Oldroyd et al. 2014; Oerlemans and Grisogono 2002). Both in deep and in shallow katabatic flows a well-developed jet, and strong shear below, is usually expected.

Factors affecting the strength and structure of the flow The ambient stratification has a key impact on the development of the katabatic winds. With strong ambient stratification, the wind speed exhibits little systematic variation in the along-slope direction and reaches a state close to local equilibrium. On the other hand, weaker stratification is associated with

along-slope increase of heat deficit and of the fluxes of downslope momentum, and a slight deepening of the flow layer (Haiden and Whiteman 2005). Based on local stratification, Arrillaga et al. (2018) suggested to classify katabatic events into three main categories, namely weak, moderate and intense, according to the observed maximum wind intensity until around midnight. Weak winds, identified by maximum speeds below 1.5 ms^{-1}, develop when either large-scale wind opposes the flow, or weak radiative cooling delays the onset of the wind. This situations are typically associated with weakly stable or neutral stratification and are characterized by a positive feedback between the weak turbulence and the cooling of the surface, which induces an increasingly stable stratification leading to a very stable regime. Stronger winds typically occur over drier soils and under favourable large-scale winds. These factors favour an earlier onset around sunset, when the stratification is still unstable, and allow the wind shear to increase without being damped by stable stratification. Due to the strong turbulence, the downward heat flux compensates the radiative surface cooling, and the thermal inversion remains limited to a thin layer close to the surface, leading to near-neutral conditions and to the development of a weakly stable layer. Moderate flows and their impact on the surface layer turbulence have not yet been fully assessed (Arrillaga et al. 2018).

Other factors, such as slope angle α and cooling heat flux, play a major role in determining the maximum depth of the flow and the wind speed. Cuxart et al. (2020) suggested a criterion to estimate the maximum depth D_{max} of a katabatic flow layer as:

$$D_{max} = -\frac{H}{v\gamma \sin\alpha}, \tag{1}$$

where H is the turbulent heat flux, v the speed of the flow along the slope, and γ the vertical gradient of ambient potential temperature.

Impact of different terrain configurations Conceptual schemes of slope winds are usually referred to ideal plain slopes, but most natural inclines exhibit non negligible curvatures. As a consequence, closely following the topographic shapes, slope flows may develop patterns alternating convergence and divergence. The effects of curved topography on katabatic winds are discussed by Haiden and Whiteman (2005), moving from the observation that at different heights above the terrain katabatic flows follow different topographic gradients. In fact, the skin flow characterizing the lowest levels above ground follows the local topographic gradient, while the bulk katabatic flow above is oriented with the larger-scale slope.

Princevac and Fernando (2007) suggests a straightforward analytical connection between flow features and topography: in the absence of significant turbulent entrainment, the downslope flow velocity u is related to the slope length L, slope angle α, and the buoyancy jump between the current and the background atmosphere Δ as:

$$U = \lambda_U \, (\Delta \; L \; \sin\alpha)^{1/2}, \tag{2}$$

where λ_U is a constant. Also, on very long slopes, the flow depth h turns out to be proportional to $L(\tan\alpha)^{1/2}$. Effects of different terrain configurations outlined through numerical simulations will be discussed in Sect. 3.

In general, katabatic flows are quite sensitive to the slope angle: Table 3 summarizes the height z_j and the intensity u_{max} of the jet, for different slope angles α, from a variety of field campaigns.

As the slope angle represents a key factor for the position of the jet, observational results will be reviewed separately for gentle and steep slopes.

Table 3 Main characteristics of katabatic wind events observed on steep and gentle slopes

Slope angle (°)	z_j (m)	u_{max} (m s^{-1})	References
Steep slopes			
21	0.5–2.0	2.0–3.0	Charrondière et al. (2020)
30–41	< 1.5	1.0–2.0	Nadeau et al. (2013), Oldroyd et al. (2016)
30	0.2–1.2	2.0–4.0	Charrondière et al. (2020)
Gentle slopes			
9	6.0	1.0–2.0	Papadopoulos and Helmis (1999)
4	40.0	3.9–4.0	Monti et al. (2002)
1.6	15.0–20.0	4.0–6.0	Whiteman and Zhong (2008), Haiden and Whiteman (2005)
2–4	4.0-5.0	2.0–3.0	Grachev et al. (2016)
1	50.0	4.0–6.0	Savage III et al. (2008), Stiperski et al. (2020)

Gentle slopes Katabatic winds developing over gentle slopes (i.e. $\alpha \sim 4° - 6°$) tend to be quite deep ($h \approx 100 - 150$ m), with jets at 10–15 m above ground and intensities around 5–6 ms^{-1} (Whiteman and Zhong 2008; Savage III et al. 2008; Haiden and Whiteman 2005; Monti et al. 2002). Similar wind speeds are observed over slightly steeper slopes, but with more shallow layers and lower jets ($z_{jet} \approx 3 - 5$ m AGL) (Grachev et al. 2016; Oldroyd et al. 2016).

The jet develops in the first two hours after sunset (Whiteman and Zhong 2008). Especially in the case of winds developing over the sidewalls of a narrow valley, later in the night the flow weakens while the down-valley flow strengthens and expands to take up more of the valley atmosphere and ambient stability increases in the lower valley with the buildup of a nocturnal inversion (Whiteman and Zhong 2008; Savage III et al. 2008). The synoptic wind conditions have large impacts on the downslope flow: in particular, opposing ambient winds lead to a shallower slope flow layer, and a smaller horizontal extent (Savage III et al. 2008). The jet maximum speed and the downslope volume flux increase with downslope distance (Whiteman and Zhong 2008).

In deep katabatic flows, jet maxima are embedded within the strong elevated inversion layer (Stiperski et al. 2020; Poulos et al. 2000; Monti et al. 2002; Heinemann 2004; Zhong and Whiteman 2008), while the stability in the near-surface inversion is significantly weakened, and the wind turning with height can be particularly strong. On the contrary, shallow katabatic flows (Oldroyd et al. 2014; Grachev et al. 2016) are mostly uni-directional and jet maxima are found at the top of the near-surface inversion, capped by weaker stability. However, the stronger differences between deep and shallow katabatic winds are found in the turbulent structure above the jet: in deep ones, the fluxes are close to zero, while in the shallower ones, a well developed turbulence is observed (Grisogono and Oerlemans 2002; Grachev et al. 2016; Oldroyd et al. 2016).

Distributed temperature sensors (DTS) based on optical fibers allowed a multiscale analysis of the near-surface katabatic temperature field from sub-meter to kilometer scale: with increasing temporal and spatial scales, slope angle and downslope distance become the most important spatial variables and the katabatic wind speed at a given location along the slope is the result of both local and basin-scale contributions, both of which evolve in magnitude followig the progression of the shade front (i.e., the transition between daylight and shade) passage (Drake et al. 2021).

Flows observed in the Meteor Crater during the METCRAX experiment (Lin-Lin et al. 2014) are a particular case of near surface winds developing over the sidewalls of an enclosed basin. Acting as a shelter, the crater allows the formation of cyclical up and downslope winds along its eastern and western sidewalls. Wind velocities appear to be lower during nighttime than during daytime. Also, they display a peak velocity extremely close to the crater's surface, indicating a very shallow slope flow layer.

Steep slopes Oldroyd et al. (2014) and (Hang et al. 2021b) performed a thorough analysis on data from measurements taken by Nadeau et al. (2013) on the 35.5° slope in Val Ferret (Switzerland) during the Slope Experiment near La Fouly ($\alpha = 25° - 45°$), and by Charrondière et al. (2020, 2022) on the 30° slope in Belledonne Mountain (France). In all cases the jets were located below 2.0 m AGL, in agreement with heights predicted by Prandtl (1942) model. Nadeau et al. (2013) identified in the wind profiles a "skin flow", a very shallow katabatic flow that forms locally and rarely exceeds a few metres in depth. Above the skin flow, a layer of downvalley wind, presumably originating from the side valley (westerly winds), was also occasionally observed.

Similar measurements were performed in Belledonne Mountain, over a snow-covered surface. Instruments included an innovative multi-hole pitot-type probe ("cobra") operated at very high sampling frequency (1250 Hz). This device allowed measuring turbulent velocity fluctuations down to 3 cm AGL (Charrondière et al. 2022). Such unprecedented observations showed that the slope normal velocity is actually far from being negligible, and raised questions on the choice of the coordinate systems used to represent these flows. Again using the data collected on the Belledonne Mountain site, Charrondiere et al (2022) were able to prove that the mean velocity of the katabatic flows increases with downstream distance s according to s^n with $n \leq 1/2$ depending on the ambient stratification. Moreover, they identified an equation for the mean wind velocity expressing its dependency on the buoyancy flux, related to the surface heat flux to the ground, entrainment and friction velocity.

Katabatic winds over glaciers Katabatic winds developing over glaciers represent a major category in the subject of thermally drive slope flows. Experiments show that these flows are recurrent and persistent, and are associated with very stable boundary layers (VSBLs) (Parmhed et al. 2004). Understanding the main characteristics of the VSBL flows and their turbulent structure is crucial for the study of glacier response to climatic changes. Hence many studies on glacier katabatic winds focused on retrieving vertical profiles of turbulent variables and fluxes and documenting their evolution in time (Denby and Smeets 2000; Oerlemans and Grisogono 2002; Van Der Avoird and Duynkerke 1999). Field campaigns were also motivated by the validation of numerical (Parish and Cassano 2003; Grazioli et al. 2017) or analytical models (Parmhed et al. 2004). Data collected over the Vatnajokull Glacier (Iceland) during the summer 1996 were used to verify the ability of a modified Prandtl model (described in Sect. 4.1) to simulate the near-surface gradients of the katabatic flow (Parmhed et al. 2004). The Prandtl model was also used to develop a simple method to estimate the sensible heat flux associated with the glacier wind, where the turbulent exchange coefficient is set to be proportional to the wind speed and the jet height (Oerlemans and Grisogono 2002). Numerical approaches were required to investigate the role of katabatic fluxes within the large scale Antarctic wind regime (Parish and Cassano 2003) and in the Arctic ice mass balance (Grazioli et al. 2017).

Renfrew and Anderson (2006) analyzed over 2600 katabatic wind profiles taken with Doppler sodars in Antarctica between 2002 and 2003 and found a systematic relation between the shape and depth of the katabatic jet and the wind speed. In fact, strong flows, with

maximum velocities of 8–10 ms^{-1} displayed a deep (up to 200 m) maximum between 20 and 60 m AGL, while moderate flows, i.e. with maximum velocities of 4–8 ms^{-1}, were characterized by shallower layers ($\approx$ 100 m) and lower jets (3–30 m). A backing of the wind direction with height was observed in all cases, consistently with decreasing friction away from the surface. Also, the strongest katabatic flows displayed a stronger cross-slope component, which is consistent with the combined effects of Coriolis force and frictional drag (a fuller account of Coriolis effect on katabatic flows will be given in Sect. 4.2.3).

The observation of katabatic winds over either clean or debris-covered ice patches in the same glacier allowed new insight into processes of glacier–atmospheric energy exchange. Glacier katabatic winds rapidly decay over the debris-covered ablation zone and the episodic intrusion of up-glacier winds from the valley below indicate the effects of katabatic winds on temperature distribution differently for the exposed and debris-covered parts (Nicholson and Stiperski 2020).

Anabatic winds

The literature on observations of daytime slope winds is less extended than for their nocturnal counterpart. Even more than for katabatic flows, the characteristics of anabatic winds are strongly marked by the topographical features and surface properties of the underlying terrain. Their inherent rapid variability under changing incoming solar radiation and ambient conditions was observed both on steep slopes in narrow alpine valleys (Van Gorsel et al. 2003; Rotach et al. 2004) or near broad plains (Reuten et al. 2005; Monti et al. 2002), and on gentle slopes over isolated mountains (Geerts et al. 2008) or on mountain ridges (Hilel Goldshmid et al. 2018).

Anabatic winds typically exhibit a more clear periodicity then katabatic winds, as the timing of their development is strongly controlled by the external forcing of solar radiation, rather than by free surface cooling. Also, unlike stably stratified downslope winds, exhibiting small vertical exchanges, daytime upslope flows are associated with convectively-driven turbulence, triggered by ground heating, and up- and downdrafts associated with convection lead to higher variability of wind direction (Monti et al. 2002).

Anabatic flows develop quite gradually during the early morning, and later attain a full development with average wind speeds of 3–5 ms^{-1} (Van Gorsel et al. 2003; Reuten et al. 2005; Monti et al. 2002) and depths up to 500 m (Reuten et al. 2005; Monti et al. 2002). During the morning, a return flow, exhibiting comparable strength and depth, is generally observed above the slope flow layer. Initially the return flow is located above the CBL, but later, in the full development, it is observed within it. Moreover, the depth of the upslope flow layer and the return flow layer aloft are each approximately half the full depth of the CBL (Reuten et al. 2005).

Van Gorsel et al. (2003) focused on the different flow structures above and below a forested canopy, and on the interaction of the slope circulation with the valley wind. Slope and valley winds interact on different spatial and time scales leading to complex patterns of momentum transport, significantly different from those over flat terrain. A full account of thermally-driven winds over forested slopes will be given in Sect. 4.2.1.

Geerts et al. (2008) studied upslope flows in connection to pressure perturbations over an isolated mountain in Santa Catalina Mountains (Arizona). Both diurnal and nocturnal flows were found to be in phase with the diurnal variation of the horizontal pressure gradient, and pointing towards the mountain during the day and away from it at night.

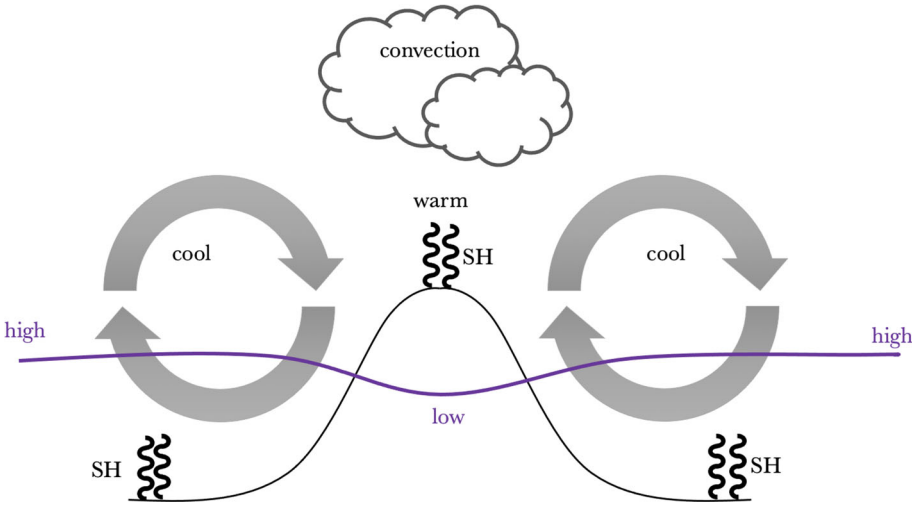

Fig. 8 Schematic depiction of the thermally forced circulation over a heated mountain under quiescent ambient conditions (adapted from Geerts et al. 2008)

2.2.3 Transitional Phases

The daily cycle of anabatic/katabatic winds implies two transitional phases around sunrise and sunset respectively. These transitions are quite challenging, both from a modelling and from an observational perspective, for different reasons: (i) they develop on times shorter than the full daytime and nighttime phases, hence they are more difficult to capture, even with multi-instrumental coordinated measurements; (ii) they result from a quite small unbalance of forcing factors, such as net radiation flux at the surface, when turning across zero from upward to downward; (iii) the turbulent regime is significantly non stationary, alternating fully convective, close to homogeneous and isotropic conditions, to remarkably heterogeneous and intermittent states.

Evening transition The beginning of the transition may be identified from several elements: the reversal of the net radiation around sunset, the reversal of the surface sensible heat flux, or the onset of a SBL. During the afternoon, the amount of solar energy received at the earth's surface slowly decreases, followed by the sensible heat flux, weakening turbulence production and initiating the afternoon transition, which is completed when the heat flux becomes definitely negative (Sastre et al. 2015). Papadopoulos and Helmis (1999) and Brazel et al. (2005) identified the main features of the evening transition from pioneering observations in complex terrain: (i) continued weak upslope flows persisting 3–5 h after sunset, delayed transition; (ii) unsteady local stagnation and vertical mixing within tens of meters above the surface; and (iii) transition of stagnation fronts to downslope and downvalley gravity currents during the evening hours, especially at higher-elevation (steeper) slopes. These studies highlighted the sensitivity of the transition mechanisms to several factors, such as valley wind speed, turbulence structure and soil moisture. These factors were later explored by means of uni- and multi-variate statistical analyses (Jensen et al. 2017). Local ambient elements effecting slope winds were also analyzed, comparing observations of the transition phase taken at different locations, in Spain and France, significantly different for heterogeneity, degree

of terrain wetness, and proximity to mountains (Sastre et al. 2015). Counter-gradient heat fluxes during the transitions were also detected by Blay-Carreras et al. (2014), and explained observing that the last eddies form during the sensible heat flux reversal: the motions of the last eddies is slowed down by turbulent viscosity and thermal diffusivity.

More recent studies concentrated on the mechanisms driving the transition. Fernando et al. (2013) proposed two prototypical mechanisms: (1) the *sliding slab*, i.e., a simultaneous stagnation and onset of the downslope flow along the entire slope, and (2) a *transition front*, i.e., the formation of a stagnation front travelling down the slope, lifting the weakening upslope-flow layer from the slope surface. The latter is based on a slope-flow evening-transition model developed by Hunt et al. (2003). Indeed, downward-traveling transition fronts were actually observed in various cases, such as the Phoenix basin (Arizona) (Brazel et al. 2005; Pardyjak et al. 2009), on a gentle northwest-facing slope of Tussey Ridge (Pennsylvania) (Mahrt et al. 2010), and on Mt. Hymettos (Greece), where the shadow propagated down the slope (Papadopoulos and Helmis 1999). In contrast, Nadeau et al. (2013) in Val Ferret (Switzerland) observed an upward-propagating flow transition on a west-facing slope with the shadow moving upslope. Furthermore, Villagrasa et al. (2013) found an almost simultaneous transition at two sites on the short slope of Meteor Crater and identified a connection between the transition time and the decay of daytime convection and turbulent kinetic energy (TKE). Likewise Lehner et al. (2015) observed that on Granite Mountain during the MATERHORN experiment the different phases characterizing the transition closely follows the propagation of a shadow front, moving down the sidewall and is followed by a 3–4 h period of almost steady-state BL conditions, with a shallow slope-parallel surface inversion, and a downslope flow exhibiting a jet maximum in the surface-based inversion.

The role of the spatial scale on drainage cooling rate during the transition was investigated by Drake et al. (2021) using DTS. The new technique allowed the investigation of an unprecedented range of temporal and spatial scales, and showed how shortly after the evening arrival of the shade front, the local cooling reached a maximum value, then decayed exponentially, and then transitioned to a linear cooling rate with time.

Morning transition Fewer studies covered the morning transition. Papadopoulos and Helmis (1999) investigated large-scale mechanisms associated with this phase in deep, idealized valleys, whereas Nadeau et al. (2020) focused on the local processes occurring close to the surface on a steep slope in an Alpine valley. Observations outlined peculiar features, such as an extreme variability in duration (from few minutes to more than one hour) and the existence of a quite long *morning calm period* (Nadeau et al. 2020). Two different competing mechanisms control the transition, and the associated inversion breakup at the foot of the slope: (i) the warming of the air from above through mixing with (replacement by) the overlying air (top-down dilution), or (ii) the warming of surface air from below due to surface heating (Papadopoulos and Helmis 1999). More recently, analysing data from MATERHORN measurements, Farina et al. (2023) investigated the conditions leading one mechanism to prevail over the other, in connection with the erosion of the nocturnal temperature inversion in an adjacent valley. They identified the ratio between the turbulent sensible heat fluxes on the valley floor and over the slope to be a crucial factor.

2.2.4 TKE and Fluxes

Katabatic flows Despite strong near-surface thermal stratification, the large shear under the katabatic jet secures a continuous source of TKE production (Monti et al. 2002; Grachev et al. 2016). Based on turbulent momentum flux, Charrondière et al. (2020) identified three

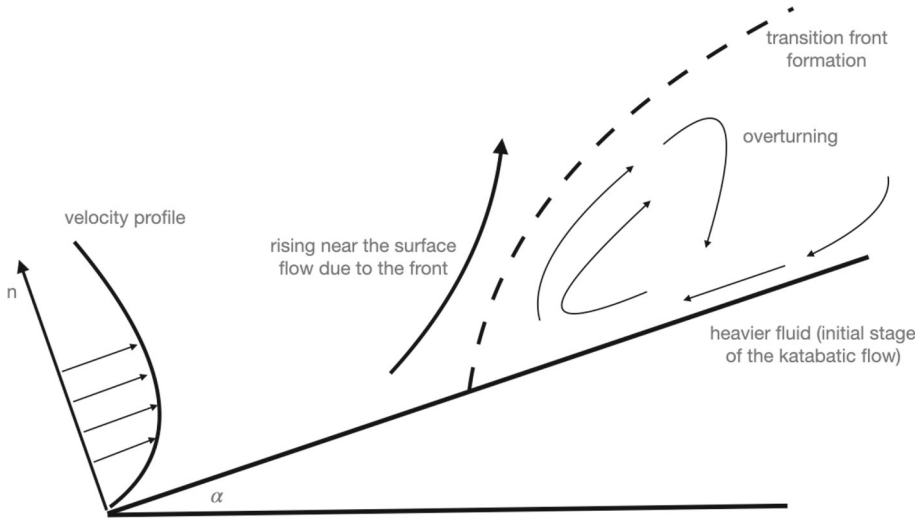

Fig. 9 Schematics of the mechanisms for the evening transition between daytime upslope and nighttime downslope flow, showing the formation of stagnation event at a slowly moving slope front and the lifting of cool air followed by local mixing (after Hunt et al. 2003) (Adapted from Brazel et al. (2005))

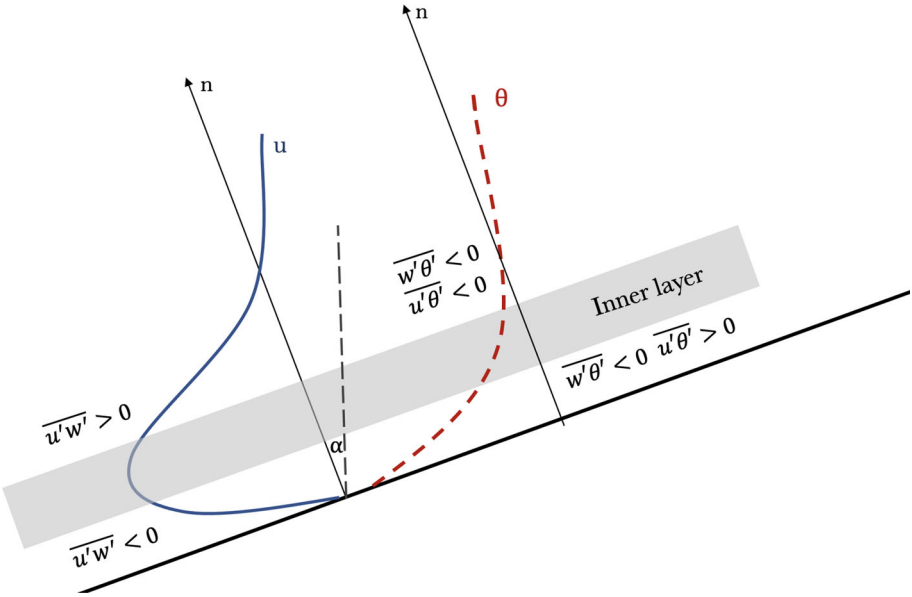

Fig. 10 Schematics of the coordinate system, fluxes, main layers and vertical profiles of wind-speed and temperature for a katabatic wind over a slope with inclination α (adapted from Charrondière et al. 2020)

regions in the vertical structure of the katabatic layer: the *surface layer*, closer to the ground, the *inner layer* around the wind jet maximum, up to the height where the momentum flux reverses, and the *outer region* above (Fig. 10).

However the most relevant features of the turbulent katabatic layer are found near the jet peak (Finnigan et al. 2020; Grachev et al. 2016; Hang et al. 2021b). All the standard

deviations of wind-speed components and the dissipation rate of TKE exhibit a local minimum there, whereas the temperature standard deviation exhibits an absolute maximum. Momentum fluxes assume contrasting values, i.e. positive above and negative below it, and so do the slope-parallel fluxes of heat and buoyancy (Grachev et al. 2016). In particular the positive slope-parallel buoyancy fluxes below the jet peak indicate a warming flux down the slope, whereas their negative values above the peak reveal a cooling flux down the slope. This vertical structure has implications on TKE profiles: buoyant production or suppression of TKE by the vertical buoyancy flux affects both stream-wise and surface-normal components of the velocity variances.

Above the jet the vertical variability is smaller than below: here turbulence is quite decoupled from the surface, as suggested by several elements, such as the zero wind shear, the change in the sign of momentum flux, the local minimum in TKE and dissipation rate, and the background stable stratification (Parmhed et al. 2004; Grachev et al. 2016; Finnigan et al. 2020). A schematic representation of these characteristics is reported in Fig. 12, and real profiles measured during the METCRAX campaign and analyzed by Stiperski et al. (2020) are shown in Fig. 11.

In deep katabatic flows the turbulence structure below the jet displays many similarities with that of shallower flows, with decreasing turbulence fluxes with height. Instead, remarkable differences are found above the jet maximum, where strong stability contributes to suppress turbulence and makes it significantly anisotropic (Stiperski et al. 2020). The new technique adopted by Charrondière et al. (2022) allowed further insight in the region closer to the ground: high-resolution velocity measurements down to 30 cm AGL revealed a well-developed logarithmic profile.

Despite their extensive use in modelling, values and parameterizations of turbulent heat and momentum diffusivities, K_h and K_m are still a subject of debate for both stable and unstable situations (Monti et al. 2002, 2014). In particular, their calculation raises concerns related to the simultaneous occurrences of either negative or positive mean shear and the vertical flux of horizontal momentum, which produce negative (and so non physical) eddy diffusivities Monti et al. (2014). The computation of K_m and K_h using the data collected during the BLLAST experiment, showed their relatively little variability during the day (Blay-Carreras et al. 2014). Moreover, the relation between eddy diffusivities and the gradient Richardson number Ri_g shows that: (i) K_m is nearly constant with Ri_g for the weakly stable regime, and then it slightly decreases for the transition regime, while slightly increases for the strongly stable regime; (ii) K_h follows a rather different dynamics, in which a marked lowering of K_h with increasing Ri_g is seen in the transition regime (nearly one order of magnitude), possibly due to the increasing role of internal gravity waves, which sustain only little buoyancy flux; and (iii) both K_m and K_h scale well with the shear length scale and the standard deviations of vertical velocity fluctuations (Monti et al. 2002, 2014). Moreover, the inverse turbulent Prandtl number $Pr^{-1} = K_h/K_m$ drops markedly as Ri_g increases, corroborating the growing evidence that the assumption of $Pr \sim 1$ is not met for strongly stratified flows (Monti et al. 2014). More recently, Charrondiere et el (2022), usin data from the Belledonne Mountain campaigns, observed that turbulent fluxes of momentum and heat depend on the stratification, expressed by the gradient Richardson number, that varies in the outer region (above the velocity maximum) from approximately 0.08 to 1.2. The ratio K_m/K_h decreases with increasing Ri, but is by a factor of approximately 1.5 larger than previously measured in a stably stratified atmospheric boundary layer, while it compares well with ratio of eddy coefficients measured in the gravity current by Odier et al. (2009) at $Ri \sim 0.08$. Their results also show that in the outer region, above the jet, both eddy coefficients and mixing lengths increase linearly with height. And such feature, together with the near log variation

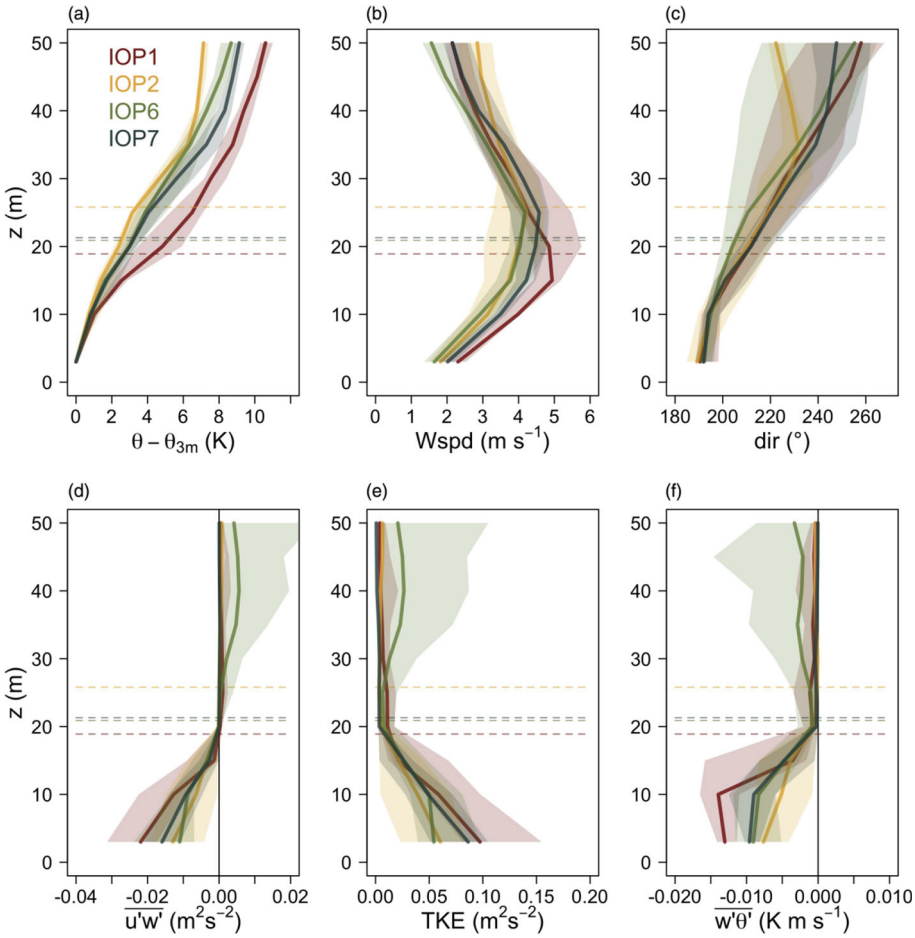

Fig. 11 Median profiles of **a** reduced potential temperature (potential temperature minus the value from the lowest level), **b** mean wind speed, **c** wind direction, **d** streamwise momentum flux in the direction of the wind at the jet maximum, **e** turbulence kinetic energy, and **f** slope-normal kinematic sensible-heat flux for selected IOPs. Horizontal dashed lines represent the medians of the jet maximum height for each IOP calculated from the fitted profiles (taken from Stiperski et al. 2020)

of the mean velocity near the velocity maximum is an interesting characteristic flow structure typical of katabatic winds on steep slopes.

Anabatic flows Observations of the structure of anabatic flows through ground-based instruments appear more challenging than for katabatic flows due to the deeper layers typically associated with the former. Hence many aspects are still less understood (Hocut et al. 2015; Weigel and Rotach 2004; Hilel Goldshmid et al. 2018; Van Gorsel et al. 2003).

Hilel Goldshmid and Liberzon (2020) provided a first analysis of the turbulent characteristics of anabatic flows by means of a sonic-hot-film combo anemometer.The increase in time of the mean intensity of the flow is linked to a decrease of the turbulence intensity and by an increase of the TKE. Moreover, both the TKE and the turbulence intensity display a linear dependency to the on the Kolmogorov scale Reynolds number Re_η.

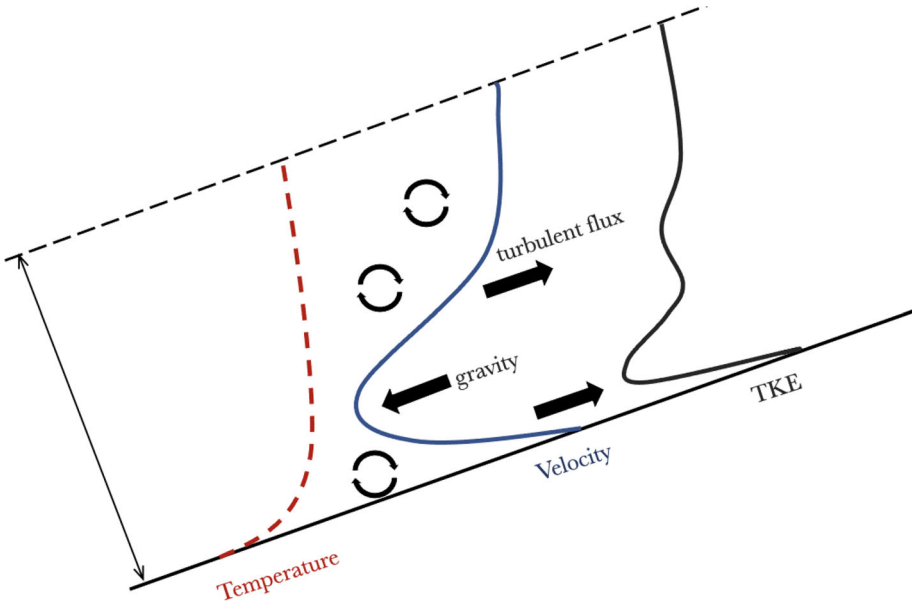

Fig. 12 Schematic representation of the vertical profiles of wind speed, temperature and TKE in a katabatic flow together with the idealized representation of the turbulent fluxes in action. Turbulence is most active below and above the slope flow core (adapted from Skyllingstad 2003)

The experimental results were compared with a theoretical model for fully developed locally isotropic turbulence using a Kolmogorov universal scaling of a one-dimensional spectra. The spectral shapes were found to fit the model in the inertial sub-range remarkably well.

Investigations in the steep and narrow Riviera Valley under fair weather summertime conditions showed that the TKE scales well with the convective velocity scale w_*, especially if calculated with the surface heat fluxes measured on the slope, rather than on the valley floor (Weigel and Rotach 2004). This characteristic seems to be connected to the significant site-to-site differences in incoming solar radiation, leading to a substantial spatial variability in the surface fluxes.

Van Gorsel et al. (2003) investigated the effects of a canopy layer on a forested valley sidewall and interactions with other circulations. They found that the second-order moments decrease with height and directional shear causes lateral momentum transport of the same order or even larger than the longitudinal ones. Further results from this study are reported in Sect. 6.1.

2.2.5 Budgets

Momentum budget The bulk momentum balance, obtained through the integration of the equations in a slope-following coordinate system from the ground surface to the top of the slope flow layer, is helpful to understand the basic mechanisms of slope flows. The momentum budget for the downslope component, neglecting Coriolis, can be written as

(Haiden and Whiteman 2005; Stiperski et al. 2020):

$$\frac{\partial \overline{u}}{\partial t} = -\overline{u}\frac{\partial \overline{u}}{\partial s} + g\frac{\Delta\theta}{\theta_0}\sin\alpha - \frac{1}{\rho_0}\frac{\partial \overline{p}}{\partial s} - \frac{\partial \overline{u'w'}}{\partial n} + R, \tag{3}$$

showing how the storage term is determined by the advection, buoyancy, pressure gradient and momentum transport. Under strong ambient stratification, buoyancy is found to be balanced by friction and the flow is close to the local equilibrium assumed in the classical Prandtl model (Whiteman et al. 2004). The flow is forced by negative buoyancy oriented down the slope, caused by the near-surface temperature deficit. Both momentum flux toward the surface and pressure gradient act to retard the flow near the surface, leading to the jet structure (Poulos et al. 2000; Stiperski et al. 2020). When the flow is unsteady and the non-zero storage term increases in magnitude with height for the shallower case, an increase of both wind strength and of its oscillations is observed (Stiperski et al. 2007).

Kossmann and Fiedler (2000) evaluated in detail the diurnal cycle of the momentum budget of the along-slope wind component near the surface with respect to the driving forces, i.e. buoyancy and pressure gradient force, and friction. They found that a small imbalance between forcing and friction is responsible for the diurnal change in the wind intensity. The along-slope components of the horizontal pressure gradient force and the buoyancy force are shown to have the same order of magnitude. As a side result, the reaction time of the slope flow to changes in forcing was then estimated to be in the range of 30 to 120 s, confirming the empirically known fact that slope winds react very quickly. In momentum budget a key role is played by pressure gradients. Haiden (2003) performed a careful analysis on how these combine with buoyancy effects and proposed a revised conceptual diagram of the relationship between buoyancy and pressure forces within the slope wind layer. In particular he showed that along-slope accelerations due to the horizontal and vertical perturbation pressure gradients cancel each other exactly if the temperature perturbation is constant along the slope.

Surface energy budget The SEB over slope is linked to several factors, such as the sun elevation angle and the state of the vegetative cover (Matzinger et al. 2003; Georg et al. 2016). The non-closure of SEB was observed in several experiments, such as the MATERHORN and METCRAX campaigns (Hoch and Whiteman 2010; Hang et al. 2016; Massey et al. 2017; ?) and improvements in terms of budget closure were investigated considering the effect of correcting net radiation on the energy balance closure in sloping terrain (Hammerle et al. 2007; Hiller et al. 2008; Serrano-Ortiz et al. 2016). Georg et al. (2016) investigated the effects of this correction, showing that it is indeed necessary, but a simpler approach based on the average inclination and aspect within a circle of 200 m radius around the flux is sufficient.

TKE budget TKE plays a major role in defining the energetics of slope winds. A simplified TKE equation, assuming along-slope and span-wise homogeneity, and neglecting moisture, can be written (Cuxart et al. 2002; Oldroyd et al. 2016; Stiperski et al. 2020):

$$\frac{\partial e}{\partial t} = \frac{g}{\theta_0}(-\overline{u'\theta'}\sin\alpha + \overline{w'\theta'}\cos\alpha) - \overline{u'w'}\frac{\partial \overline{u}}{\partial n} - \overline{w'^2}\frac{\partial \overline{w}}{\partial n} - \frac{\partial \overline{w'e'}}{\partial n} - \frac{1}{\overline{\rho}}\frac{\partial \overline{w'p'}}{\partial n} - \epsilon + R. \tag{4}$$

In the above equation the buoyancy production by the streamwise heat flux (term 1) is generally negligible for small slope angles (Oldroyd et al. 2016); Stiperski et al. 2020), while the production from the slope-normal heat flux (term 2) is negative for katabatic flows and

balances production of TKE. Shear production associated with the streamwise (term 5) and spanwise momentum fluxes is quite relevant, especially for deep katabatic winds (Stiperski et al. 2020; Oldroyd et al. 2016). where e is the the TKE, epsilon is the dissipation and R is the residual.

In general, negative contributions (suppressing TKE) are found in the vertical buoyancy term, while the the slope-parallel buoyancy fluxes can be both negative or positive (Finnigan et al. 2020).

Unlike for flat terrain, the along-slope component of the kinematic heat flux contributes to the vertical buoyancy flux:

$$\frac{g}{\theta}\overline{w_z'\theta'} = \frac{g}{\theta}(-\overline{u'\theta'}\sin\alpha + \overline{w'\theta'}\cos\alpha), \tag{5}$$

where w_z is the vertical velocity component, whereas w is the slope-normal velocity component.

Observations show that for katabatic flows over steep-slopes the positive contributions from the along-slope component are greater than the negative contributions from the slope-normal component, resulting in a positive vertical buoyancy flux and production of TKE despite the near-surface statically stable stratification stratification(Oldroyd et al. 2016). From (3) it is clear that buoyant production of TKE over sloping terrain occurs when:

$$\frac{\overline{u'\theta'}}{\overline{w'\theta'}} > \cot\alpha. \tag{6}$$

Remarkably, this is in contrast with classical ABL theory for horizontal terrain, where static stability is associated with negative buoyancy fluxes and suppression of TKE. Moreover, farther from the ground ($z \geq 20\,m$) the TKE budget terms show negligible turbulence generation or destruction, but their ratio shows the dominance of buoyancy suppression (Stiperski et al. 2020). From the analysis of measurements over a glacier in Greenland Heinemann (2002) showed that the profile of the dynamical production of TKE has the same shape as the TKE itself and TKE destruction by negative buoyancy is very small.

For scales under 10 min, the pressure transport term (term 6) is of the same order of magnitude as the others and is not well correlated with any of them, whereas above 10 min, the pressure transport term results significant and tends to be compensated by the turbulent transport term at the same scales, the other terms of the budget being of smaller orders of magnitude (Cuxart et al. 2002). Finally, turbulent dissipation (term 7), balances the turbulent production by other terms, and it is highlighted that the residual term (8) is small but non-zero so the balance is not closed.

Heat flux budget The stream-wise heat flux budget is defined as:

$$\frac{\partial\overline{u'\theta'}}{\partial t} = +g\frac{\overline{\theta'^2}}{\theta_0}\sin\alpha - \overline{w'\theta'}\frac{\partial\overline{u}}{\partial n} - \overline{u'w'}\frac{\partial\overline{\theta}}{\partial n} - \frac{\partial\overline{w'u'\theta'}}{\partial n} + R, \tag{7}$$

and the evaluation of the different terms from measurements shows similarities with the TKE budget (Stiperski et al. 2020) such as the negligible contributions of production terms over a certain height above ground. This seems to be caused by non-local sources of stream-wise heat fluxes. Within 20 m AGL, the vertical wind shear and vertical temperature gradient are the main contributors. The budget is also significantly under-closed (Stiperski et al. 2007; Haiden and Whiteman 2005). Moreover, differences between the deep and shallow katabatic flows can be found in terms of the role of the temperature gradient term, which has stronger

effects in the shallow case, due to the higher near-surface stability. The turbulence suppression due to buoyancy does not seem to play a significant role, contrary to results for steeper slopes.

Budgets during the transition The momentum and TKE budgets are particularly relevant during the transition phases. Kirshbaum (2013) showed that the shear production of TKE is negligible in the last two hours before the evening transition, while the buoyant production of turbulence dominates the TKE budget and experiences a sudden decrease exactly at sunset. At night, the mechanical production overpowers the buoyant consumption of turbulence by a factor of 1.7. The buoyancy term remains positive throughout the transition period resulting in a net positive vertical buoyancy flux. Considering the momentum budget, during local sunrise the buoyancy acceleration drives the flow under the katabatic regime, while it is less important under the diurnal upslope regime (Nadeau et al. 2020).

2.3 Laboratory Scale Experiments

Laboratory water tanks can be a useful tool to study flows over heated or cooled sloping surfaces immersed in a stratified fluid. However scaling them appropriately through dimensional analysis is not trivial. Hence results from them need to be evaluated very carefully before inferring conclusions on larger scale processes.

Reuten et al. (2007) investigated layering, venting and transport of pollutants by upslope flows in a bottom-heated, salt-stratified water tank over a slope between an adjacent plain and a plateau, under various configurations. They observed how trapping effects are favoured under weak large-scale flows, strong sensible heat flux, weak stratification. Similarly, Princevac and Fernando (2007) performed laboratory simulations in a V-shaped tank containing thermally stratified water. On the uniformly heated sloping surfaces, they observed that upslope flows leave the sidewalls and intrude horizontally into the stratified fluid over the valley center, flowing up the slope as a bentover plume and not rising vertically. Flows became turbulent as soon as the heat flux becomes large enough and can be sustained only above a minimum slope angle that turned out to be only 0.1° for average atmospheric conditions (Princevac and Fernando 2007).

Baines (2001) investigated katabatic flows in stratified environments in laboratory tanks introducing a continuous source of negatively buoyant fluid at the top of a constant-angle slope ($\alpha = 20°$). They found that the flow maintains a uniform thickness and a distinct boundary at its top, until it approaches neutral buoyancy and leaves the slope, while flows of negatively buoyant fluid over steep slopes are in the form of entraining plumes (Baines 2005). Real downslope flows over valley sidewalls are not produced by a continuous source of negatively buoyant fluid at the top of the slope. Rather, they lose heat continuously to the underlying surface to maintain their negative buoyancy. Nevertheless, laboratoryanalogs provide important information on the processes occurring at the slope layer's top. Hunt et al. (2003) used a laboratory tank to study the evening transition to katabatic flows for a gentle slope for which the length of the sloping plane far exceeds the thickness of the CBL. The transition was induced subjecting the upslope flow to a rapidly changing surface flux. The analysis confirmed that the flow reversal occurs at a finite distance along the slope with the appearance of a front, which then migrates down the slope.

Moroni et al. (2014) simulated both anabatic and katabatic flows in a vessel filled with distilled water to simulate the circulation in the surroundings of an urban area in a mountain valley. They showed that in anabatic flows, eddy structures form and move upslope, while in katabatic flows the depth of the flow layer increases towards the slope base. The urban-

heat-islandslope- flow interaction was also investigated by of Shindler et al. (2013), through an advanced hybrid Lagrangian technique. The results identified a dependence of the mean quantities on different slope heating and significant effects on the circulation in the large city located on the valley floor.

Various lab-tank studies investigated factors controlling the upslope-flow separation (Hocut et al. 2015; Broekema et al. 2020; Hilel Goldshmid et al. 2018). This occurs when the BL loses contact with the associated confining wall, which is usually caused by a pressure gradient acting against the local flow direction. This process is crucial to predict strong updrafts and deep convection. Broekema et al. (2020) outlined the possibility of two different flow states over steep slopes: (i) a vertically attached flow combined with horizontal convergence, and (ii) a vertically detached flow combined with horizontal divergence. On a similar line Hilel Goldshmid et al. (2018) focused on the sensitivity analysis of parameters such as the width of the plateau, the slope angle, and the heating rate, following the work of Hocut et al. (2015), who identified three different regimes for the formation of a rising plume separated by two critical values of the slope angle.

3 Numerical Modelling

3.1 Reynolds Averaged Navier Stokes (RANS) models

Slope winds were simulated using a variety of numerical models, such as the Regional Atmospheric Modelling System RAMS (Renfrew 2004; Poulos et al. 2007; Zhong and Whiteman 2008; Lehner and Gohm 2010), the Advanced Regional Prediction System ARPS (Chemel et al. 2009; Trachte et al. 2010; Serafin and Zardi 2010b; Trachte and Bendix 2012), the Coupled Ocean/Atmosphere Meso-scale Prediction System COAMPS (Söderberg and Parmhed 2006) and LOVECLIM (Barthélemy et al. 2012).

A substantial part of the above studies focused first on the simulation of katabatic flows on large ice sheets, in the attempt of reproducing long time series of data from observations in the Arctic (Bromwich et al. 2001) and Antarctic regions (Klein et al. 2001). The investigation was later extended to unveil the role of katabatic winds in specific polar phenomena, such as the dynamics of polynya (Ebner et al. 2014) and blue ice areas (Zwinger et al. 2015) in Antarctica, or wind and temperature structure over a melting glacier (Söderberg and Parmhed 2006) and surface-atmosphere exchange processes driven by katabatic winds (Spall et al. 2017). Renfrew (2004) investigated katabatic flow dynamics in a particular topographical configuration, i.e. a moderate slope and the adjoining ice shelf, using five years of climatic data collected in the Coats Land in Antarctica and obtaining an accurate description on the katabatic layer dynamics, including sources of internal gravity waves. The impact of the topographic configuration was investigated by Trachte et al. (2010) using idealized terrain models reproducing the eastern Andes area. The simulations showed that, in a lowland basin with a concave terrain-line, confluence of katabatic flows may occur, and a complex drainage flow system directed into such a basin can sustain the confluence katabatic flows in a lowland basin with a concave terrain-line occur, and that a complex drainage flow system regime directed into such a basin can sustain the confluence despite varying slope angles and slope distances.

The analysis of upslope flows within the development of the CBL over an idealised plain-slope-plateau system highlighted peculiar features, such as the occurrence of a transient depression at the base of the slope and the formation of elevated turbulent layers above the

CBL (Serafin and Zardi 2010a). Similar elevated turbulent layers were later shown to be produced by the overturning towards the valley center of slope winds associated with the morning development of a CBL in idealised valleys (Serafin and Zardi 2010b). The resulting CBL thermal structure of the inner valley was then shown to be shaped quite different than above an adjacent plain. This contrast between thermal structures plays, in turn, a key role in the build-up of the along-valley pressure gradient driving valley winds (Serafin and Zardi 2011).

Mesoscale heat transport was the focus of the simulations performed by Noppel and Fiedler (2002) with the non-hydrostatic model KAMM, including atmospheric and soil vegetation sub-models describing the interaction between soil, canopy and the overlying air. They found that slope winds promote a mesoscale vertical transport of sensible heat, which has a considerable impact on the atmosphere even above the PBL height. This vertical transport has a magnitude comparable to the turbulent flux at the same height, but is much more organised, since its patterns are closely connected to the underlying topography. Hence Authors recommend to duly account for it in global climate models.

Martínez and Cuxart (2009) compared the output of a hydraulic model with results from a high-resolution mesoscale model simulations of katabatic flows in the Northern Spanish plateau, finding that the former captures the basic mechanisms driving the flows, but was not able to close the budget equations, as the residuals remained quite large.

Mesoscale modelling proved to be a useful tool to investigate the interaction of slope winds with other atmospheric structures such as mountain waves (Poulos et al. 2000, 2007) and valley inversions (Zhong and Whiteman 2008), as well as their role in moist processes, such as the formation of convective clouds (Trachte and Bendix 2012). In particular, Oltmanns et al. (2015) focused on the special case of recurrent downslope winds in Ammassalik (Southeast Greenland) reaching hurricane intensity, and representing a hazard for the local population and environment. They simulated two specific wind events, a stronger and a weaker one, with WRF, and tested different model and topography resolutions, ranging from 1.67 km to 60 km.

Despite their influence on coastal processes and on the deep ocean properties, katabatic winds are generally poorly represented in global climate models. In particular, the associated wind stress is strongly underestimated. Hence Barthélemy et al. (2012) developed a correction for wind stress modifications in the vicinity of the Antarctic coast, based on comparison with atmospheric surface circulations simulated by a regional model. The improved representation of katabatic winds resulted in a thinner sea ice layer and in a enhanced production of it along the continent, in better agreement with observations.

3.2 Large-Eddy Simulations

In Large-eddy simulations (LES) of turbulent flows only the larger energy-containing eddies are explicitly resolved, whereas the unresolved smallest eddies are parameterized. However, the size of these "smallest eddies" may be significantly different for katabatic and anabatic winds: the energy-containing eddies are typically smaller in size in SBLs than in convective ones. Accordingly, numerical simulations of katabatic winds require finer grids and longer computational times. This may partly explain why earlier LES experiments focused on upslope flows (Schumann 1990), whereas simulations of downslope flows started much later (Skyllingstad 2003; Smith and Skyllingstad 2005; Axelsen and van Dop 2009a, b; Largeron et al. 2010; Burkholder et al. 2011; Schmidli 2013; Smith and Porté-Agel 2014; Brun 2017) and for idealized slopes only.

Skyllingstad (2003) simulated the flow on a steady surface cooling in a neutrally stratified ambient atmosphere obtaining mean vertical profiles of velocity and temperature quite comparable with observations. On the same basis, Smith and Skyllingstad (2005) simulated the flow developing over a surface consisting of an upper steeper slope and a lower gentler one. Results show a rapid acceleration over the upper steeper slope, followed by a transition to a slower evolving flow with an elevated jet over the lower gentle slope. Similarly, Zhong and Whiteman (2008) focused on katabatic flows over a gentle slope and their connections with valley inversions. Their sensitivity analysis suggests that an increase in the downvalley winds leads to a decrease in the maximum downslope wind speed, and to a deeper downslope wind layer. Further progress in the simulation of katabatic flows, and in evaluating their sensitivity to environmental parameters, was made by Axelsen and van Dop (2009a, b). Comparison with measurements from two glaciers showed a good agreement for first order moments, but significant discrepancies in the buoyancy and momentum fluxes. Furthermore a sensitivity analysis and a comparison with two versions of Prandtl models—respectively with constant K and with z-varying K (Grisogono and Oerlemans 2001)—proved how they can reproduce many features of the vertical profiles of velocity, buoyancy and momentum fluxes, the major differences being mainly due to the crude approximations implied by constant K. From the TKE budgets, it was shown that the wind shear is the largest production term and is mainly balanced by turbulence dissipation, while near the wind maximum, where the shear vanishes, the turbulence transport is the only production term. A similar comparison between LES results and the Prandtl model was later proposed by Grisogono and Axelsen (2012). Their results suggest that both the maximum wind speed u_{max} and its height z_j decrease with increasing slope angle α, whereas in Prandtl (1942) solutions only the latter is affected by α. A linear relation between the z_j and u_{max} is found, which is supported by observations. The mixing properties of the katabatic flow layer were also discussed by Largeron et al. (2010), who showed that the katabatic flow is non stationary, and mixing is quantified by a turbulent (thermal) diffusivity ($0.01 - 2\ m^2\,s^{-1}$) depending on atmospheric stability, in agreement with measurements from field campaigns. They also found a dependence of the turbulent diffusivity $\overline{K_t}$ on the Froude number Fr associated with the katabatic flow:

$$\overline{K_t} = C_k Fr^2, \tag{8}$$

with $C_k = 0.015\ m^2\,s^{-1}$ and $Fr = u_{max}/(NL)$, L being the distance from the ground at which the amplitude of the along-slope velocity becomes lower than $u_{max}/100$.

An overview of the main features of LES experiments reported in the literature for katabatic flows is shown in Table 4.

Concerning the definition of the wall layer vertical gradients of velocity and buoyancy, those are usually determined from Monin-Obukhov theory (MOST), although its inadequacy for the simulation of katabatic flows has been suggested in different studies (Grisogono and Oerlemans 2001; Grisogono et al. 2007). In particular, when the L_{MO} is larger than the height of the jet, L_{MO} is not able to capture the effects of turbulent eddies on the fluxes. Grisogono et al. (2007) proposed a modified version for L_{MO} that includes also the jet height. However later Axelsen and van Dop (2009b) assessed that the proposed correction term is negligible, allowing them to apply the standard MO theory in the wall layer.

The analysis of the interaction between the slope flows and valley winds and their role in heat exchanges showed that the net effect of the thermally induced cross valley circulation is to export heat out of the valley, while from a local perspective the slope-flow-induced subsidence leads to a warming of the air in the valley center (Schmidli 2013). Catalano and Cenedese (2010) simulated the entire diurnal cycle of the circulation over a slope in simplified and idealized conditions, focusing on valleys with strong capping inversion. The

Table 4 Summary of the main features of the Large Eddy Simulations performed to study katabatic flows

Study	SGS model	$\Delta h(m)$	$\Delta z(m)$
Skyllingstad (2003)	FSF	0.75	0.75
Smith and Skyllingstad (2005)	FSF	2.5	2.5
Smith and Skyllingstad (2005)	TKE 1.5	100	5
Zhong and Whiteman (2008)	TKE 2.5	250	2.1
Axelsen and van Dop (2009a)	TKE	2.6	0.4
Burkholder et al. (2010)	Multiple	2.17	2.17
Catalano and Cenedese (2010)	TKE 1.5	50	2
Largeron et al. (2010)	–	200	5–98
Grisogono and Axelsen (2012)	TKE	2	0.4
Smith and Portè-Angel (2013)	Multiple	5–20	1.−3.3

Subgrid Scale (SGS) model, the horizontal (Δh) and vertical Δz grid steps. FSF stands for Filtered Structure Function model

model reproduces the circulation dynamics driven by the thermal forcing, with the diurnal growth of the CBL associated with the development of anabatic winds on the valley sidewalls and the growth of cold pools during night along with katabatic flows. Brun (2017) simulated a katabatic jet along a convexly curved slope with a maximum angle $\alpha_{max} = 35.5°$, finding that advection and production contributions to TKE in the downslope direction are not negligible along curved slopes. They also found substantial centrifugal accelerations leading to the emergence of Gortler vortices, and a significant departure from isotropy.

LES of katabatic flows also allowed testing different sub-grid scale (SGS) models. Burkholder et al. (2011) tested SGS performance in reproducing turbulence statistics and spectra in katabatic flow. They found that the performance of the basic SGS closures is acceptable for mean fields, but fails to reproduce higher-order moments, in particular buoyancy fluxes. Smith and Porté-Agel (2014) extended the previously cited study to shallower slopes and included a Lagrangian scale-dependent dynamic model to determine possible critical limits to the grid resolution and grid isotropy ratio, which may hinder accurate LES modelling of katabatic winds. Their results show that downslope fluxes of mass and buoyancy deficit are highly sensitive to SGS closure choice. Furthermore, the use of scale-dependent dynamic models suggest that the assumptions of scale invariance are violated and predictions of vertically integrated downvalley mass and buoyancy fluxes are more sensitive to vertical than horizontal grid resolution.

For anabatic flows, in the last two decades Cintolesi et al. (2021) provided the only contribution specifically focusing on LES, after the pioneering work by Schumann (1990). They identified three dynamic layers: the near-surface *conductive layer*, the *convective layer* where the most energetic motions develop, and the *outer region*, almost unperturbed. Moreover from inspection of instantaneous fields they detected the development of thermal plumes, i. e. stable turbulent structures, which contribute to enhance the vertical transport and mixing of both momentum and heat.

3.3 Direct Numerical Simulations (DNS)

Direct numerical simulations (DNS) resolve explicitly all scales of the governing equations. As such, with the available computational resources nowadays they can simulate turbulent

flows up to moderately high Reynolds numbers. Earlier successful attempts mostly focused on nocturnal katabatic flows (Shapiro and Fedorovich 2007; Fedorovich and Shapiro 2009; Shapiro et al. 2012; Fedorovich et al. 2017; Umphrey et al. 2017), and some also considered the diurnal component (Fedorovich and Shapiro 2009; Giometto et al. 2017). The effects of non-uniform surface heating was investigated by Shapiro and Fedorovich (2007) considering the cooling induced by an isolated strip and by Shapiro et al. (2012) for local surface cooling. The comparison with the results obtained with an analytical model showed consistent differences among them, especially in the position and magnitude of the jet. Moreover, the investigation of the role of the Coriolis force shows how a laminar flow induced by a cold strip of finite width running down the slope reaches a steady state in which buoyancy fields and cross-slope winds vanish far above the slope (Shapiro and Fedorovich 2007).

The analysis was pursued further by Hewitt R. and A. (2023), who found two modes of temporal instability; stationary down-slope aligned vortices and downslope propagating waves. By considering the limiting inviscid stability problem, they showed that the origin of the vortex mode is spatial oscillation of the buoyancy profile normal to the slope, leading to vortex growth in a region displaced from the slope surface, at a point of buoyancy inflection. They also found that Rayleigh waves dominate in general, but the vortex modes become more significant over gentle slopes. Shapiro and Fedorovich (2014) adopted a more sophisticated analytical and mathematical approach including the test of a new scaling based on two non dimensional parameters, i. e. Prandtl and Reynolds numbers. Here the slope angle does not appear as an independent governing parameter, but acts as a stretching factor in the scales for the dependent and independent variables and appears in the Reynolds number.Advances in the techniques for the simulation of both laminar and turbulent slope flows are proposed by Umphrey et al. (2017) through the investigation of a cartesian-mesh immersed boundary formulation within an incompressible flow solver. First order statistics of the turbulent flow are noticeably sensitive to the specific formulation of the immersed boundary, although the scheme works better for laminar than for turbulent flows. Shapiro and Fedorovich (2007) and, more recently, Giometto et al. (2017) simulated the entire daily cycle (reaching Grashov number $Gr \approx 10^{11}$), including both the diurnal and nocturnal components and provided a deep analysis of the first and second order turbulent moments of the flow. Turbulent anabatic and katabatic regimes show identical structure for the vertical wall set-up, but undergo a different transition in the mechanisms sustaining turbulence as the sloping angle decreases, especially for very low slope angles. Moreover, budget analysis shows how the mean KE is fed into the system through the imposed surface buoyancy, and then redistributed by turbulent fluctuations from the LLJ nose towards the boundary and outer flow regions. The TKE budget equation also suggests a subdivision of the boundary layer of both anabatic and katabatic flows into four distinct regions: (i) an outer layer where turbulent transport is the main source of TKE and balances dissipation; (ii) an intermediate layer, bounded below by the LLJ and capped above by the outer layer, where the sum of shear and buoyant production overcomes dissipation, and where turbulent and pressure transport terms are a sink of TKE; (iii) a buffer layer where TKE is provided by turbulent and pressure transport terms, to balance viscous diffusion and dissipation; and finally (iv) a laminar sub-layer, where the influence of viscosity is significant.

4 Analytical Modelling

4.1 Exact Solutions for Steady Flows: Prandtl (1942) and Beyond

The well-known pioneering Prandtl's (1942) model offered a basis for many subsequent developments. The model represents a steady balanced wind flowing over an infinite slope, tilted by an angle α with respect to the horizontal, as a result of a constant surface heat flux, prescribed in terms of a constant surface temperature anomaly ΔT_s, uniformly distributed along all the slope length, in a stably stratified ambient atmosphere, otherwise at rest, with Brunt-Vaisala frequency N. Solutions for the along-slope wind velocity u and the potential temperature anomaly θ are:

$$u(n) = U\mathrm{e}^{-\frac{n}{l}} \sin\left(\frac{n}{l}\right) \quad \theta(n) = \Delta T_s \mathrm{e}^{-\frac{n}{l}} \cos\left(\frac{n}{l}\right), \tag{9}$$

where n is the slope-normal coordinate, $U = N\gamma^{-1}Pr^{-1/2}\Delta T_s$ is a velocity scale, g is the acceleration due to gravity, γ is the vertical gradient of potential temperature in the unperturbed atmosphere, and $Pr = \nu/k$ the Prandtl number, whereas the length scale l is:

$$l = \left(\frac{4k\nu}{N^2 \sin^2\alpha}\right)^{1/4}. \tag{10}$$

The above solutions represent the basic physical mechanisms implied by the momentum balance between along-slope advection and cross-slope turbulent fluxes of potentially warmer/colder air by down-/up-slope flows respectively, and the cross-slope heat flux associated with thermal conductivity. Nevertheless, some remarkable limitations can also be noticed in this scheme. For example, the scale length l, controlling the slope-normal structure of the velocity and temperature anomalies, turns out to be independent from a key quantity such as the surface heat flux. Also, it grows indefinitely when either the slope angle or Brunt-Vaisala frequency decrease, becoming singular in the limiting cases of either horizontal terrain or neutrally stratified ambient atmosphere respectively. Moreover, the velocity scale U is remarkably independent from the slope angle α.To overcome these and other limitations preventing the application of the above solutions to realistic situations various authors suggested suitable extensions or modifications.

4.1.1 Constant K

Defant (1949) extended Prandtl model to turbulent flows, simply replacing viscosity and heat diffusivity with their eddy counterparts, to reproduce observations from wind velocity measurements on the Nordkette (near Innsbruck, Austria). The comparison was party satisfactory, with poorer agreement for up-slope winds. To improve the performance of the extended Prandtl model, Grisogono and Oerlemans (2001) adopted a gradually varying K(n). The resulting steady-state solution, calculated by means of the WKB method, exhibits a more realistic shape, and compares better with data from measurements over the Pasterze Glacier (Austria). Similarly, Giometto et al. (2017) generalized the closed-form solution proposed by Nieuwstadt (1983) for the stationary Ekman layer to reproduce katabatic flows with a spatially-varying eddy viscosity and diffusivity.

Spoeck and Arbeiter (2021) pursued further the WKB method, with a different approach: prescribing slope angle, Prandtl number and turbulent quantities u_* and θ_*, as well as the form of the eddy thermal diffusivity function K_H, they identified the corresponding WKB Prandtl

model. Also, they investigated the connection between u_* and θ_* calculated via MOST over horizontal terrain and those associated with a turbulent slope flow.

4.1.2 Alternative Closures

Mo (2013) suggested a parameterization of turbulent momentum and heat fluxes by means of linear terms, proportional to velocity, through a Rayleigh friction coefficient k_T, in the momentum equations, and to potential temperature anomaly, through a Newtonian cooling coefficient k_N, in the heat equation respectively. The resulting analytical solutions do not suffer from any singularity, for either $\alpha = 0$ or $N = 0$.

Similarly, moving from a simple K-closure approach, Łobocki (2017) performed an analysis of second-order moment budget equations. Based on the concept of turbulent potential energy introduced by Zilitinkevich et al. (2007, 2008), he identified pathways of exchange between potential energy of mean flow and total turbulent mechanical energy. In particular, he showed that this process is controlled by the inclination of the potential temperature gradient.

4.1.3 Nonuniform Surface Heating/Cooling

Shapiro et al. (2012) analysed the katabatic flow driven by a non-homogeneous surface forcing in the form of a "cold strip", where the surface buoyancy flux varies down the slope as a "top-hat" profile. They obtained an analytical solution for steady-state linearized governing equations, exhibiting a primary Prandtl-like katabatic jet, a rotor-like feature straddling the upslope end of the strip, and two nearly horizontal jets: an inward jet of environmental air feeding into the primary jet on the upslope end of the strip and an outward jet resulting from the intrusion of the primary katabatic jet into the environment on the downslope end of the strip. Numerical results confirmed linear solution, but also outlined some minor differences.

4.1.4 Nonlinear Effects

In Prandtl (1942) model the governing equations are remarkably linear: assuming parallel flow and invariance with the along-slope coordinate removes nonlinear advection terms from momentum and heat equations.

Ingel'L (2000) introduced a nonlinear term through the closure of the boundary conditions for momentum and heat fluxes at the surface, and found a continuously growing layer depth and velocity in time.

Grisogono et al. (2015) and Güttler et al. (2016, 2017) also questioned the assumption of linearity for significantly stratified situations. Accordingly, they suggested to include in the advection term of the heat equations an additional contribution from the slope-normal gradient of the temperature perturbation. Through a weakly-nonlinear perturbation approach they derived a correction to the basic Prandtl solution, which compared better with observations.

4.2 Analytical Solutions for Special Cases

4.2.1 Similarity and Scaling

Within the scientific community quite a general consensus seems to exist concerning the limits of Monin-Obukhov similarity theory (MOST) in reproducing the observed profiles of slope

winds. In fact, the grounds of MOST fail to be met for a slope surface layer: in particular, it can hardly be detected a layer exhibiting turbulent fluxes invariant with distance from the surface (Denby and Smeets 2000; Charrondière et al. 2020). Accordingly, other scaling laws were investigated. Nadeau et al. (2013) found that MOST was not applicable due to large variations of the turbulent fluxes with height in the lowest 5–6 m of the surface layer. Tests on the applicability of local scaling were promising for flux–variance relationships of the slope-normal wind velocity component, the temperature and the specific humidity, and more so under convective conditions. However, after removing the effects of self-correlation, the slope-parallel velocity fluctuations did not show any relationship with the measurement height and the local Obukhov length. In the neutral limit, they found $\sigma_u/u_* \sim 2.85$ and $\sigma_v/u_* \sim 2.24$ slightly above previously reported values. Also, observations did not support the classical Businger–Dyer expressions for the non-dimensional profiles of wind speed ϕ_m and temperature ϕ_h. The discrepancy was greatest under statically stable conditions. Such deviations from traditional similarity theory were mostly attributed to three factors: (i) advection from the slope wind preventing a constant-flux layer, (ii) negative wind-speed gradients due to shallow drainage flows close to the surface, and (iii) a misalignment of the coordinate system with the gravity vector.

From numerical simulations by means of a second order closure model, Łobocki (2014) showed that the classic MOST profiles may be used with almost no modification under unstable equilibrium, with simple geometric adjustments to account for the direction of the surface stress and for scaling the distance to the surface. However, in stable conditions, modifications of the universal functions ϕ_m and ϕ_h are also necessary. These can be quite simple for downslope winds over gently or moderately sloping terrain. However, the model results for upslope flows over steep terrain point to a more complex behaviour.

Sfyri et al. (2018) investigated the structure of standard deviations of temperature and humidity from measurements at six sites with different slope angles, orientation and roughness in the i-Box experimental site (see Sect. 2.1). They screened several assumptions at the basis of MOST, including turbulence fluxes invariance with height and self-correlation among the turbulence variables, and found that some basic assumptions for MOST applicability were violated. Therefore they concentrated on a local similarity hypothesis. The scaled standard deviations as a function of local stability were compared with previous studies from various combination of both horizontal and non horizontal, homogeneous and (weakly) inhomogeneous, as well as truly complex terrain. Results for temperature variances indicates that the best-fit functions for every site are different, and these differences are statistically significant. Nevertheless, some similarities are found between the sites over the steepest terrains. Hang et al. (2021a) proposed a modified flux-gradient relation for wind shear below the jet peak in the form $\phi_m = 0.65\zeta_\alpha^{0.56} + 0.67$, where $\zeta_\alpha = (n - d_0) / (\tan\alpha\ \Lambda)$.where Λ is the local Obukhov length. On a similar basis, Grisogono et al. (2007) questioned the use of MOST for katabatic flows, and proposed, as an alternative length scale, the jet height:

$$z_j = \frac{\pi}{4}\left(\frac{4K^2 Pr}{N^2 \sin^2\alpha}\right)^{1/4}. \tag{11}$$

Accordingly, they introduced a modified scale resulting from the combination of the two:

$$L_{MOD}^{-1} = aL_{MO}^{-1} + bz_j^{-1}, \tag{12}$$

where a and b are coefficients to be determined from observations and K is the eddy heat conductivity. The non-dimensional number $Br = (L_{MO}/z_j)^2$ can be used to discriminate when either scale is most appropriate, as shown in Fig. 13.

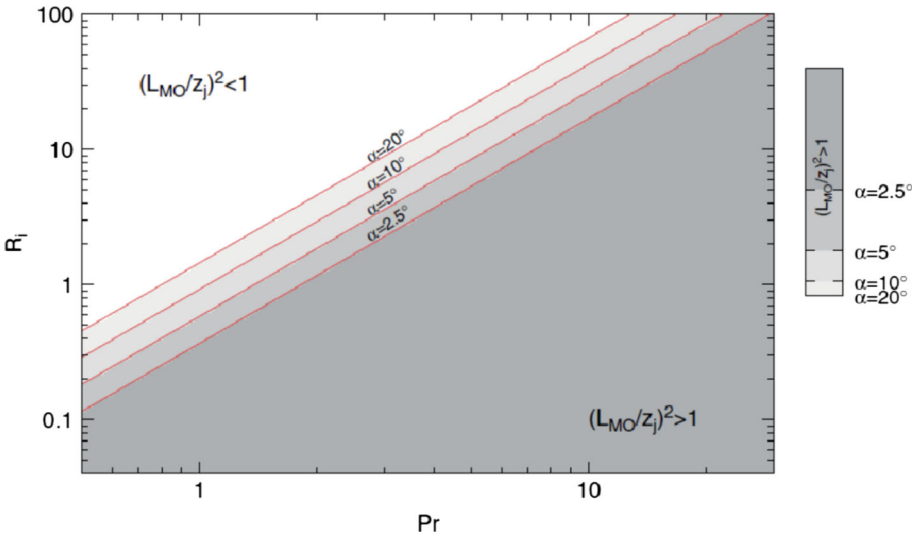

Fig. 13 Log-log display of the squared ration of the Monin-Obukhov length vs the low-level katabatic jet height, $Br = (L_{MO}/z_j)^2$ for four different values of terrain slopes. Whenever the ratio is larger than one, $Br > 1$, pertaining to the lower right part of the plot, L_{MO} is not the relevant scale for the near surface turbulent fluxes. Higher the slope and/or stronger the stratification, earlier the onset of $Br > 1$ and hence the validity of the proposed scaling. Reproduced from (Grisogono et al. 2007)

On the same line, Stiperski et al. (2020) investigated the relatively deep and persistent katabatic flows developing on a gentle mesoscale slope with a long fetch (~ 30 km) outside the Barringer Meteorite Crater in Arizona during METCRAX II (Lehner et al. 2016), where the small slope angle causes the formation of deep flows with jet maxima ranging between 15 and 45 m AGL, and average 5 min speed at z_{jet} reaching up to almost 8 ms^{-1}. These deep katabatic flows exhibit near the surface a turbulent structure similar to that of shallow katabatic flows over steeper slopes. The fluxes (apart from the sensible-heat flux) are non-constant with height even below 10 m height, and their magnitudes decrease as z_{jet} is reached. Above z_{jet}, on the other hand, no continuous turbulence is maintained, making turbulence profiles markedly different from those of shallow katabatic flows. Differently from results found in other studies, z_jet is not the relevant length-scale determining the turbulent structure of these deep katabatic flows, and is not correlated with the maximum height to which continuous and quasi-isotropic turbulence is maintained, i. e. the SBL height, which may reach values as high as 43 m. The height of the katabatic SBL was found to depend on the same forcing mechanisms (stability profile, surface values of sensible-heat flux and friction velocity) as that of the SBL over flat terrain. Fair agreement was found with the commonly used formulations, provided the local near-surface stability was used instead of the free tropospheric background stratification. The dominant eddy length-scale from the Multi-Resolution Flux Decompositon co-spectra of sensible-heat flux, which turned out to be constant with height, offered another measure of the SBL height, which allowed estimating the katabatic turbulent depth from single-level turbulence measurements. An alternative scaling was proposed by Hunt et al. (2003) for an upslope wind developing over a gentle incline connecting two flat adjoining planes at different elevations, and longer than the depth h of the CBL developing over the slope. Combining data from field observations in winter 1998 in the Phoenix Valley (Arizona, USA) and from laboratory experiments, they noted that flow disturbances induced by the initiation of the

upslope flow propagate into the adjacent plains at the long-wave speed, accompanied by unsteady wave fronts. However long waves propagate faster than the ensuing upslope wind: hence the flow adjustments at the edges of the incline do not influence the upslope flow establishment, and the process may be considered as driven by a constant heat flux under steady state. Accordingly, assuming surface heating with a fixed heat flux, the upslope flow develops in time and achieves a quasi-steady state wherein the characteristic velocity scale can be written as $U_M = \alpha^{1/3} w_*$, where $w_* = (F_{bs} h)^{1/3}$, with F_{bs} being the surface buoyancy flux.

4.2.2 Non-stationary Slope Winds

The extension of Prandtl model to allow for non-stationary conditions is straightforward, once tendencies for both velocity and temperature are included in the governing equations, as first suggested by Defant (1949). Based on this scheme, Zardi and Serafin (2015) investigated the time-periodic flows developing over an infinite slope undergoing a surface temperature cycle with angular frequency ω, in an overlying stably stratified ambient atmosphere. They identified two distinct flow regimes, and showed that the vertical structures of wind speed and temperature depend on two length scales:

$$l_+ = \sqrt{\frac{2K}{N \sin\alpha + \omega}} \quad l_- = \sqrt{\frac{2K}{|N \sin\alpha - \omega|}}. \tag{13}$$

A supercritical regime occurs when $N \sin\alpha > \omega$ (i.e strong ambient stability and steep slope). Under this regime the vertical structure of temperature and velocity perturbations is very similar to the steady Prandtl flow, but oscillating in time with the same cycle of the driving surface temperature, as shown by Defant (1949). Instead, in the sub-critical regime profiles of u and θ deviate considerably from those suggested by Prandtl theory. In particular the response of upper layers to the surface forcing may be strongly delayed by a significant phase shift. A notable example of a real situation where this may happen is that of nearly neutral ambient atmosphere, such as in the late morning and afternoon stages of the diurnal cycle of mountain breezes, when anabatic flows occur in a weakening stratification due to the formation of an ambient mixed layer (Serafin and Zardi 2010b). Hence slope-normal profiles of temperature and wind speed should not be expected to match the Prandtl model, even approximately, in these situations.

4.2.3 Extension to Rotating Frame of Reference and Including Coriolis Effects

Earth rotation negligibly affects thermally driven winds in mountainous regions, whereas it may affect large scale, long-lived katabatic winds over large iced surfaces in polar regions. Stiperski et al. (2007) calculated both analytical and numerical solutions of Prandtl model for these cases. They found that the steady Prandtl model including Coriolis force is not equivalent to its time dependent counterpart, even after long time periods. While the two slope-parallel velocity components – U downslope and V orthogonal to U—reach a steady state after the typical time-scale for simple katabatic flows $T \sim \frac{2\pi}{N sin\alpha}$, changes in V diffuse upwards in time without a well-defined time-scale. Hence V may even affect the circumpolar stratospheric vortex after a few months of polar night.

5 Stability and Oscillations

5.1 Instabilities in Prandtl Slope Flows

Prandtl model for down-slope flows is susceptible to different types instabilities which can be studied using linear modal analysis, as well as numerical simulations (Senocak and Xiao 2020). Such instabilities are controlled by three dimensionless parameters, suggested by Buckingham Pi theorem: the slope angle α, the Prandtl number and Π_a, a stratification perturbation parameter.

Hence Senocak and Xiao (2020) explored the instabilities arising in different conditions in katabatic flows using a combination of linear modal stability analysis and a DNS.

The Prandtl model for katabatic slope flows results prone to both transverse and longitudinal modes of instability (Xiao and Senocak, 2019): the transverse modes promote stationary vortical structures aligned in the along-slope direction, whereas the longitudinal modes of instability emerge as waves propagating along-slope. The two modes coexist and form complex structures crossing the plane of the flow. For $\alpha \leq 62°$ a stationary, 3D mode of instability, characterized by longitudinal vortex rolls, can be triggered. For higher slope angles, a 2D wave instability develops and travel along the slope, due to the stronger along-slope component of gravity in such a configuration.

A similar stability analysis was performed for katabatic flows over an infinite and uniformly cooled surface subject to a downslope uniform ambient wind aloft, using a modified Prandtl (Lykosov and Gutman 1972) to derive the base flow (Xiao and Senocak 2020b). A linear analysis shows that, for a fixed Prandtl number and slope angle, two independent dimensionless parameters are sufficient to describe the flow stability: the stratification perturbation number Π_s and the wind forcing number, that can be interpreted as the ratio of the kinetic energy of the ambient wind aloft to the damping due to viscosity and the stabilising effect of the background stratification. Depending on values of these parameters and of the slope angle, transverse and longitudinal-travelling modes of instabilities emerge.

The extension of this analysis to anabatic winds due to a uniform surface buoyancy flux showed the emergence of two different kind of instabilities: stationary longitudinal rolls, due to the component of the buoyancy normal to the sloped surface, and a Kelvin-Helmoltz mechanism travelling streamwise characterized by a shear instability modulated by buoyancy. The latter appears to be more easily developed for $\alpha \geq 9°$. So basically, the transition between the two dynamics happens at lower angles with respect to the katabatic case (where the critical values was identified in 62°). The results obtained through the linear modal analysis are confirmed by DNS (Xiao and Senocak 2020a).

The self-pairing of the stationary longitudinal vortical rolls emerging in katabatic and anabatic Prandtl flows at shallow slopes are identified as a unique flow structure (Xiao and Senocak 2022). The internal interaction of the counter-rotating vortex pair is a precursor for further destabilization and final breakdown of the flow into smaller structure and the topology of the pair results similar to speaker-wires.

5.2 Experimental Evidence of Oscillations

A remarkable feature accompanying the development of katabatic winds is the occurrence of waves associated with the flow. Indeed, the equations of highly stable katabatic flows admit slope-normal internal-waves, which were also detected from observations (Van Gorsel et al. 2003). These internal waves interact with the wind shear in the layer and generate local

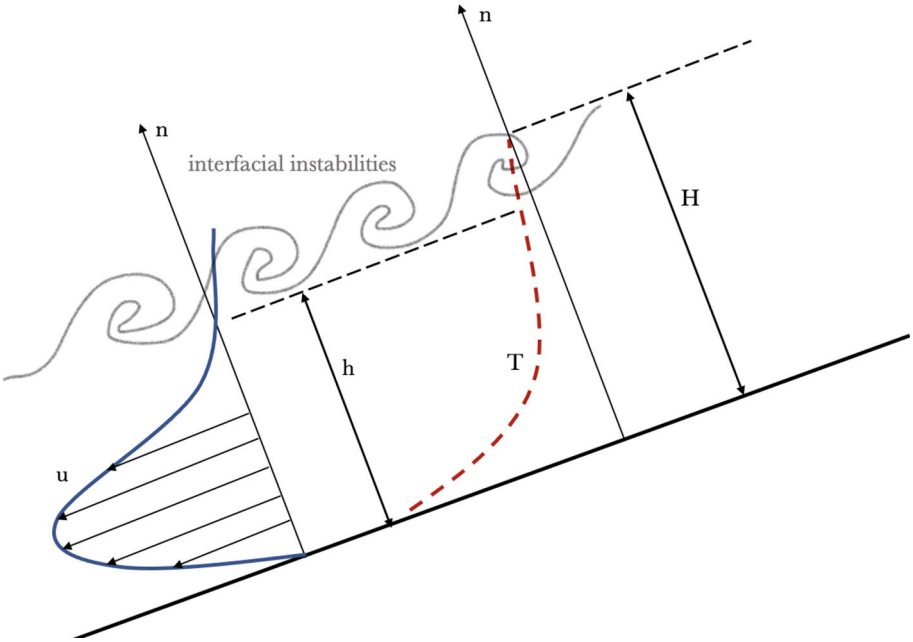

Fig. 14 Schematics of a quasi-steady katabatic current over an idealized slope: the occurrence of instabilities is highlighted in the representation (adapted from Princevac and Fernando 2007)

turbulence upon reflection from the slope (Princevac and Fernando 2007), as schematized in figure 15. Considering the layer-averaged equations for small time scales, the linear solution of the flow exhibits an oscillatory component of frequency $N \sin\alpha$, where N is the Brunt-Vaisala or buoyancy frequency. These waves, excited by background disturbances, may play a dominant role in the katabatic flow and the associated energy budget. The occurrence of gravity waves was attributed to different mechanisms. The first ever proposed is based on the action of an adverse pressure gradient generated by the air accelerating down the slope and its adiabatic heating. Parameterising friction as $F = -k\,u$, Fleagle (1950) showed that the resistance reduces as the air decelerates, while the driving force continues to be enhanced by radiative cooling, resulting in a oscillatory behavior of the flow. Another possible mechanism involves cross flows, temporarily blocking drainage currents from tributary valleys: as cold air layers form, and buoyancy forcing increases in the tributaries, sudden releases of colder air onto the slopes may occur periodically. Princevac and Fernando (2007) obtained a good agreement comparing observed frequencies from the VTMX experiment data with those predicted considering this along slope internal-wave oscillations mechanism.

Henao-Garcia et al. (2022) got insights into the mechanisms controlling oscillations in katabatic winds considering laminar flows. They observed damped oscillations to dominate the initial oscillatory stage of laminar katabatic slope flows. Stationary longitudinal rolls are dominant at shallow slopes, and are observed to meander with increasing stratification perturbation parameter and the average distance between the rolls exhibits a strong dependence on slope inclination for slope angles less than 35°. At much steeper slopes, traveling slope waves emerge and are transported at the mean jet velocity. Both types of instability rolls coexist for certain combinations of dimensionless parameters, forming intricate structures that break into smaller eddies as the flow becomes more dynamically unstable.

6 Specific Paradigmatic Cases

6.1 Slope Winds over Vegetated Slopes

Understanding wind and temperature fields within forest canopies over sloping terrain is a crucial prerequisite for appropriate parameterizations of surface-vegetation-atmosphere exchanges (Bonan et al. 2021).

Even over short vegetation thermally driven flows are likely more complex than over non-vegetated topography (Oldroyd et al. 2014; Grachev et al. 2016). A peculiar feature is the potential for buoyant turbulence kinetic energy production via slope-parallel buoyancy fluxes (Oldroyd et al. 2016). Moreover, radiative heating and cooling need to be evaluated not only near the ground, but also at the top of the canopy, and there may be multiple layers of thermally driven flows.

The interaction of slope flows with specific types of non-homogeneous canopy reveals a complex relationship between canopy organization and turbulent and mean flow dynamics. The main deviations that were observed are a downslope flow above the canopy during daytime under strong synoptic wind and, vice versa, upslope flow above the canopy during nighttime for the presence of Southerlies. These modifications resulted in either substantial amplification or attenuation of the normal flow (Feigenwinter et al. 2008). Moreover, studies performed on anabatic winds developing over steep forested slopes by Aubinet et al. (2003) and Van Gorsel et al. (2003), allowed the identification of remarkable differences form flat terrain cases: (i) upslope winds and cold air drainage display a wind speed maximum within the trunk level and, within the canopy, a sharp attenuation of turbulence occurs (ii) skewed distributions of velocity components suggest intermittent turbulent transport playing an important role in the energy distribution(Van Gorsel et al. 2003) (iii) vertical velocity at the top of the canopy was well correlated with the surface velocity under statically stable conditions (Aubinet et al. 2003). Sharp changes in the vegetation cover of the sloping terrain are determined by two contrasting mechanisms: vegetation shading and sloping bottom effects on circulation patterns. The prevalence of one over the other is linked to the kind and depth of the vegetation (Lin and Wu 2015). The vegetative cover also modifies the interaction with valley wind circulations through the decoupling of the sub-canopy layer from the above flow (Wang et al. 2015). In deciduous forests, the influences of canopy on drainage flow may be expected to be different in foliated and leaf-off seasons (Wang et al. 2015).

The presence of a vegetative canopy also influences the TKE and turbulent fluxes balances of the slope flows. Oldroyd et al. (2014) developed a one-dimensional mean momentum balance formulation to describe the katabatic jet on steep slopes covered with vegetation. Including the effect of short vegetation and weak larger-scale pressure perturbations allowed to explain the large fluctuations in wind direction. The role of a canopy was explored by Everard et al. (2020) in a sloped vineyard ($\alpha = 7°$). They found that the proximity of the jet to the canopy top adds a further characteristic turbulent transport of momentum away from the near-canopy environment.

The thermal structure developing in the forest canopy affects processes that ventilate the forest. In particular, sub-canopy inversion strength has a dual relationship to sub-canopy wind speed and moisture flux from the forest. When the daytime heating of the canopy is small and sub-canopy inversions weak, above-canopy winds mix sub-canopy air more efficiently, and lead to stronger slope-normal moisture flux and weaker along-slope advection of water vapor. On the other hand, under strong heating of the canopy top, strong sub-canopy inversions inhibit vertical moisture flux, and daytime downslope winds under the canopy are stronger.

Increased downslope advection redistributes sub-canopy water vapor and other atmospheric constituents from upslope to downslope areas (Drake et al. 2022).

Evidences of the formation of a stable within-canopy layer allowed the conclusion that horizontal mean advective fluxes are restricted to a relatively shallow layer of air beneath the canopy, with little vertical mixing across a relatively long horizontal fetch (Yi et al. 2005).

The impact of a grass canopy on the one-dimensional mean momentum balance has been explored via theory and field measurements by Oldroyd et al. (2014), finding that outer layer pressure effects can be significant under low-speed wind conditions at the top of the katabatic layer and that with tall and dense vegetation the dynamics become much more complex, as added mechanical drag and canopy–atmosphere heat transfer alters the behaviour of a drainage flow, and thus the interaction of the two flow types.

Observations made in a sloped vineyard (Everard et al. 2020) suggest that the coldest air is both advected and locally produced in the agricultural area, showing a potential for advective frost risk during times of slope drainage. However, the katabatic flow itself appears to enhance vertical mixing which could act as a countermeasure to block or deflect cold air from the steep mountain slopes from stopping in the vineyard.

The analytical representation of the very special case of katabatic wind occurring within forest canopies is not trivial. The governing mechanisms are similar to flows over simpler surfaces, with the remarkable difference that within a canopy momentum and heat budgets may depend on quite different factors (Wang et al. 2015). In particular within the canopy wind velocity and potential temperature deficit are quite uniform with height in the drainage layer. Also momentum and heat fluxes are strongly controlled by the canopy structure, and can be appropriately represented in terms of suitable bulk drag and heat transfer coefficients. Chen and Yi (2012) proposed a scheme to reproduce a balanced flow based on bulk momentum flux proportional to the squared average velocity. Based on such a scheme, they derived an analytical solution for steady katabatic wind providing an estimate of mean temperature anomaly and wind velocity. Based on these solutions, they found that optimal conditions for katabatic flows within canopies are controlled by terrain angle, canopy structure and thermal condition through a simple equation:

$$L_c V_T^{-2} \alpha = b, \tag{14}$$

where $L_c = (c_D a)^{-1}$ is a canopy length-scale, with c_D the drag coefficient and a the leaf area density, whereas $V_T = R_c/\gamma$ is a thermal factor, defined by the cooling rate R_c and $b = (2g)^{-1}[\frac{\theta_0}{(\theta_0 - \theta_c)}]$ is a constant with g being the acceleration due to gravity, θ_0 the ambient stratification and θ_c the potential temperature when the cooling rate is zero. This theoretical prediction implies that gentle slopes are optimal for katabatic flow developments in stably stratified air, while steep slopes are optimal in weak or near-neutral stratification.

6.2 Interactions with Other Meteorological Phenomena

Valley winds Over highly complex terrain dynamic interactions between slope flows and other circulations may occur. In particular, on valley sidewalls interactions of slope and valley winds are observed (Van Gorsel et al. 2003; Rotach et al. 2008; Wang et al. 2015). The flow close to the surface is generally controlled by a slope wind system while higher up the valley wind direction dominates. Observations suggest that in the first tens of meters from the surface there is a substantial influence of the slope wind system–even during the time of full development of the valley wind system (Van Gorsel et al. 2003; Rotach et al. 2008).

Mountain waves A key topic within the dynamics of thermally driven circulations is that of the interaction with mountain waves, which results to be particularly robust and significant for the katabatic component of the cycle (Poulos and Zhong 2008). The interaction between the two systems is mutually interdependent: while turbulence and pressure effects imposed on katabatic flows by mountain waves alter their structure, characteristics, and evolution, those same changes (particularly alterations to atmospheric stability) feedback and alter gravity wave evolution.

Katabatic winds below sea level: the case of the Dead Sea Katabatic winds have been studied also over the slopes surrounding the Dead Sea, located at 433 m below sea level (BSL), during the summer season, when such flows are most frequent, persistent and pronounced due to the stable weather conditions (Paperman et al. 2022). The observed flow was characterized by a katabatic layer reaching 950 m AGL. Using a wide range of instrumentation, including radiosondes and lidars, the study investigated the characteristics of the intermittent katabatic flows developing in the area, and so the wind pulses, finding out that the average direction of the pulses depends on the nearby slopes orientations while the intensity depends on the elevation and its location relative to the slope. The average katabatic number of pulses, duration, time intervals and their beginning and terminating times were found to strongly depend on the other local flows. Moreover, the average number of the katabatic pulses was found to be 2.9–3.5 pulses every night, and the average duration of each pulse was 69–94 min.

Sea breezes For mountainous areas close to the sea, a topic of interest is the interaction between slope winds and their marine equivalent, the sea breezes. Porson et al. (2007) tried to capture the dynamics of the sea-breeze circulation combined with an upslope-flow circulation, using numerical simulations. Their results show clear scaling regimes and strong interaction between the two thermally driven circulations. They identified three dynamical regimes of interaction, corresponding to different inland extents of maximum updraft velocity, depending on slope length, slope angle, stability and surface flux.

Cold pools The role of drainage flows in the formation of cold pools at the valley bottom is still a topic of active research. It is likely that katabatic flows do not actually penetrate into the cold pool but rather flow over it (Bodine et al. 2009). In particular, observations performed by Mahrt et al. (2010) showed that the drainage flow penetrates to the valley floor at the beginning of the evening, accelerating over the lower part of the slope. However, the acceleration diminishes as the cold pool thickens and occupies more of the slope. When that happens, the drainage flow can no longer penetrate to the bottom of the slope.

Convection Kirshbaum (2013) combined analytical and numerical models to simulate a two-layer flow representing the boundary layer and the overlying free troposphere over an isolated mountainlike heat source. He developed a scaling based on the linearized Boussinesq equations to quantify the strength of thermally forced updrafts and to identify three flow regimes, each with distinct dynamics and parameter sensitivities. This scaling closely matches corresponding numerical simulations in two of these regimes: the first characterized by a weakly stable boundary layer and significant background winds and the second by a strongly stable boundary layer. The third regime is characterized by weak winds and weak boundary layer stability. Here the scaling is outperformed by a fundamentally different scaling based on thermodynamic heat engines. Within this regime, the inability of wind ventilation or static stability to diminish the buoyancy over the heat source leads to intense updrafts that

are controlled by nonlinear dynamics. These nonlinearities create a positive feedback loop between the thermal forcing and vorticity that rapidly strengthens the circulation and contracts its central updraft into a narrow core. As the circulation intensifies under daytime heating, the warmest surface-based air is ventilated into the upper boundary layer, where it spreads laterally to occupy a broader area and, ultimately, restrains the circulation strength.

Fog Finally, the interaction between drainage flows and fog was studied in relation to air quality issues in the city of Zagreb. Prtenjak et al. (2018) developed a conceptual scheme for katabatic flow hydraulic jump to improve the forecast of fog in the city area. Depending on the nature of the downslope flow, if super- or sub-critical, it will be accompanied by a hydraulic jump causing it not to flow over the plain, so leaving the fog to be shallow and dense.

Orographic convection. In conditions of sufficient forcing due to solar radiation, weak stratification, and weak wind, thermally driven circulations, with anabatic flow converging over the mountain, develop. This is commonly referred to as toroidal circulation, because of the horizontal vorticity forming a ring (or toroid) around the mountain itself (Demko 2009; Geerts et al. 2008). The results of experimental observations with ground-based and aircraft-based instrumentation over a isolated mountain highlighted that mountain-scale mass convergence near the surface cannot be used as a precursor for convective initiation over mountains and that orographic cumulus vertical growth is controlled by something else, which is most likely the evolution of the profile of static stability determined by surface heating over the mountain, or by changes aloft (Demko 2009). As a matter of fact, the toroidal heat island circulation is observed, with divergence in the upper BL. It typically develops after sunrise and peaks at solar noon. The hydrostatic horizontal pressure gradient and the temperature patterns confirm that the anabatic flow is driven by surface heating over the mountain (Geerts et al. 2008). Moreover, it is observed that orographic thunderstorms suppress the BL solenoidal circulation, due to cold-pool spreading.

Urban effects Seo et al. (2017) examined the interactions of urban breezes with slope winds under a background wind and a stably stratified ambient atmosphere, and a prescribed surface thermal forcing. A mathematical model was obtained reproducing the interactions between urban breezes and slope winds through the linear superposition of individual analytical solutions for urban thermal forcing, mountain thermal forcing, and mountain mechanical forcing for a city downwind of a mountain. During nighttime, in the mountain-side urban area, near-surface flows induced by mountain cooling and mountain mechanical forcing cooperatively interact with urban breezes, resulting in strengthened winds. During daytime, in the urban area, near-surface flows induced by mountain heating are opposed to urban breezes and promote weaker winds. The degree of interaction between urban breezes and slope winds is sensitive to mountain height and basic-state wind speed. In particular, a change in the background wind speed affects not only the strength of thermally and mechanically induced flows, but also their vertical extent and decaying rate. Studies performed with WRF in the city of Almaty (Kazakhstan) showed how the formation of a heat island is tied to the wind conditions and so to the thermally driven circulations developing in the area. In particular, it is observed that Almaty's nocturnal heat island is cooler than the daylight heat island due to the katabatic wind, diffusing in the urban quarters (Zakarin et al. 2022).

6.3 Transport of Species

Transport phenomena associated with slope winds make them extremely relevant for air quality. Mountain valleys are often the location of settlements, industrial activities and major viability infrastructures and are characterized by intense emission of pollutants at ground level. The interest in the role played by thermally driven winds is determined by air quality observations suggesting that the temporal variation of pollutants' concentrations is dominated by such circulations, with only minor influences from background synoptic winds (Alexandrova et al. 2003; Pardyjak et al. 2009). While valley winds may transport pollutants deep inside the valley during daytime and cleansing during the night, up-slope flows may transport primary pollutants, or precursors of secondary pollutants, to higher levels in the atmosphere where they are subject to synoptic-scale transport, or are simply carried over to adjacent valleys. The transport of primary pollutants, or even precursors, to higher elevations may lead to high concentrations of secondary pollutants over elevated regions, where the different exposure to higher radiation levels and/or ambient conditions may affect chemical reactions and pollutant transformation. Transport by anabatic flows (*chimney effect* or *mountain venting*) is particularly strong when slope flows converge over a mountain summit (De Wekker and Kossmann 2015) or when there is an additional sea breeze flow in coastal terrain (De Wekker et al. 2004). However, observations showed how the mass transport of upslope flow and return flow is approximately balanced over a 4-h morning period (Reuten et al. 2005), suggesting a closed slope-flow circulation within the CBL making air pollutants trapped within a the slope-CBL rather than being vented into the free atmosphere.

Lehner and Gohm (2010) performed simulations of daytime pollution transport within a deep valley (an idealized version of the Inn Valley in Austria) during wintertime. They found that during periods of persistent inversion, high concentrations of during the entire day and lead to poor air quality in the valley. Finally, changes in surface albedo determined by differences in the vegetation coverage and in the snow cover are identified as the drivers of vertical changes in the stability and in the slope-wind-induced mass flux, which, in the end, produce cross-valley flows removing the tracer from the slope-wind layer (Harnisch et al. 2009; Gohm et al. 2009).

The nocturnal drainage flow of air causes significant uncertainty in carbon diozide and water vapour determined with the eddy covariance measurement approach. Measurements performed in forested sloping terrain evidenced how the horizontal and vertical advection of CO_2 plays a key role in the budget equation but at the same time its evaluation is technically and theoretically complex (Aubinet et al. 2003; Yi et al. 2005). The comparison between the measurements performed over a flat, hilly and slope site by Feigenwinter et al. (2008) showed how the vertical and horizontal advection affects all the sites during nighttime and that both the vertical and the horizontal advection are always positive in the slope site due to downslope winds. Improvements in the evaluation of the advective fluxes cannot be performed regardless of those in the understanding of the vertical and horizontal structure of the drainage flows (Yi et al. 2005), which are found to be restricted to a relatively shallow layer beneath the canopy with little vertical mixing along the horizontal. Horizontal CO_2 concentration gradient is hypothesized to be negative in convective situations and slightly positive in equilibrium situation by Aubinet et al. (2003) and this hypothesis is confirmed by the measurements of Heinesch et al. (2008). The latest advances on the topic of the interactions between katabatic flows turbulence and CO_2 concentrations are presented by Arrillaga et al. (2018): their work provides an evaluation of the one-dimensional governing equation for CO_2 between two measurement levels close to the terrain and the computation of the horizontal transport. The comparison of the advective effects of slope flows in weak and a strong katabatic events,

shows that the more intense is the event, the greater the turbulence and the higher the CO_2 mixing in the surface layer.

7 Conclusions

The amount and extent of results outline the remarkable progress made in the last two decades in our understanding of thermally driven winds developing over mountain slopes. This has been possible thanks to a series of targeted field experiments, concentrating an impressive deployment of equipment including a variety of different instruments for both ground based and airborne measurements, as well as remote sensing instruments. On the other hand, the increasing availability of high performance computational resources allowed simulating by means of numerical models fine details of the above flows at unprecedented resolution in space and time.

The katabatic winds have been more extensively explored than the anabatic ones, both in terms of experimental observations and in terms of numerical and analytical modelling, due to their increased steadiness in time and to the absence of external forcing linked to the diurnal solar activity.

Slope winds are difficult to resolve in large scale weather prediction models commonly adopted for operational global scale run, and even more so for climate projections. However, the increasingly higher resolution allowed by continuous progress in available computational resources is expected to improve the capability of the above models in reproducing such flows. Accordingly, more adequate parameterizations of surface layer processes are required to cope with these advances. Finally, the identification of new, successful, parameterizations is strongly linked to the development of new scaling laws specifically thought for complex terrain and in particular for the BL over a slope. In order to find and test new scaling laws, observational data collected in the most idealized conditions possible are needed, to be able to understand and simulate the processes in their basic and more simple form, as a first step towars understanding more complex situation in which several other external factors are also kept into account. The above reasoning claims for an extended—in time and space—major field campaign explicitly meant for the observation and understanding of pure slope winds. Indeed experiments performed so far covered part of the quantities associated with the development of slope winds, but it would be desirable to have a targeted field campaign at a nearly ideal slope. Such campaign should allow a better determination not only of the vertical structure of the wind, temperature and turbulent fluxes fields throughout the depth where turbulence is found to occur, but also of the surrounding ambient conditions, including both the free atmosphere properties and in particular stability and the nearby conditions at the edges of the slope area. Such a campaign should provide the required material to answer many questions still open, and can be summarized as follows:

- understanding connections between topography, surface properties, ambient stability and upper forcing with the dynamical and thermal structure and development of slope winds under typical situations;
- identifying turbulence dynamics and structures in thermally-driven slope flows and their role in the mechanisms controlling daytime upslope winds, nighttime downslope winds and the transitions between them;
- identifying a hierarchy in the spectrum of scales of motions activated in the various situations of slope winds, and determining how they contribute to transport and mixing

processes, especially the larger ones, in the light of the analysis suggested by Zilitinkevich et al. (2006);
- identifying suitable similarity scaling for the dynamical and thermal structure of slope winds
- assessing the role of slope flows on transport and exchange (turbulent mixing, along slope advection, entrainment, upper convection,...) at different scale: surface layer, slope layer, free atmosphere;
- understanding the effects of upper conditions (e.g. upper winds, or increasing cloud cover from convection) on the atypical development and modifications of slope low structure and evolution.

Acknowledgements Dino Zardi is deeply grateful to Prof. Sergej Zilitinkevich for his valuable teaching and warm encouragement, and in particular for the interest Prof. Zilitinkevich displayed on his work on slope flows, and the fruitful reasoning following from a stimulating discussion at the Annual Meeting of the European Meteorological Society in Trieste in 2016, and continuing during a visit of Prof. Zilitinkevich to the University of Trento in summer 2019 and a visit of Dino Zardi to the University of Helsinki shortly after. Those stimulating reasonings were part of a cooperation on a research project which should have led to a joint publication: the present article is also a tribute to all the valuable effort Prof. Zilitinkevich invested in that project.

Funding Open access funding provided by Universitá degli Studi di Trento within the CRUI-CARE Agreement.

References

Alexandrova OA, Boyer DL, Anderson JR, Fernando HJ (2003) The influence of thermally driven circulation on PM10 concentration in the Salt Lake Valley. Atmos Environ 37(3):421–437

Arrillaga JA, Yagüe C, Román-Cascón C, Sastre M, Maqueda G, Vilà-Guerau de Arellano J (2018) Weak and intense katabatic winds: impacts on turbulent characteristics in the stable boundary layer and CO2 transport. Atmos Chem Phys Discuss

Aubinet M, Heinesch B, Yernaux M (2003) Horizontal and vertical CO2 advection in a sloping forest. Boundary-Layer Meteorol 108(3):397–417

Axelsen SL, van Dop H (2009) Large-eddy simulation of katabatic winds. Part I: Comparison with observations. Acta Geophys 57(4):803–836

Axelsen SL, van Dop H (2009) Large-eddy simulation of katabatic winds. Part II: Sensitivity study and comparison with analytical models. Acta Geophys 57(4):837–856

Baines PG (2001) Mixing in flows down gentle slopes into stratified environments. J Fluid Mech 443:237–270

Baines PG (2005) Mixing regimes for the flow of dense fluid down slopes into stratified environments. J Fluid Mech 538:245–267

Banta RM, Darby LS, Fast JD, Pinto JO, Whiteman CD, Shaw WJ, Orr BW (2004) Nocturnal low-level jet in a mountain basin complex. Part I: Evolution and effects on local flows. J Appl Meteorol Climatol 43(10):1348–1365

Barthélemy A, Goosse H, Mathiot P, Fichefet T (2012) Inclusion of a katabatic wind correction in a coarse-resolution global coupled climate model. Ocean Model 48:45–54

Blay-Carreras E, Pardyjak E, Pino D, Alexander D, Lohou F, Lothon M (2014) Countergradient heat flux observations during the evening transition period. Atmos Chem Phys 14(17):9077–9085

Bodine D, Klein PM, Arms SC, Shapiro A (2009) Variability of surface air temperature over gently sloped terrain. J Appl Meteorol Climatol 48(6):1117–1141
Bonan GB, Patton EG, Finnigan JJ, Baldocchi DD, Harman IN (2021) Moving beyond the incorrect but useful paradigm: reevaluating big-leaf and multilayer plant canopies to model biosphere-atmosphere fluxes: a review. Agric For Meteorol 306(108):435
Brazel A, Fernando H, Hunt J, Selover N, Hedquist B, Pardyjak E (2005) Evening transition observations in Phoenix. Arizona. J Appl Meteorol Climatol 44(1):99–112
Broekema Y, Labeur R, Uijttewaal W (2020) Suppression of vertical flow separation over steep slopes in open channels by horizontal flow contraction. J Fluid Mech 885:A8-1-A8-31
Bromwich DH, Cassano JJ, Klein T, Heinemann G, Hines KM, Steffen K, Box JE (2001) Mesoscale modeling of katabatic winds over Greenland with the polar MM5. Mon Weather Rev 129(9):2290–2309
Brun C (2017) Large-eddy simulation of a katabatic jet along a convexly curved slope: 2. Evidence of Görtler vortices. J Geophys Res: Atmos 122(10):5190–5210
Burkholder BA, Fedorovich E, Shapiro A (2011) Evaluating subgrid-scale models for large-eddy simulation of turbulent katabatic flow. In: Quality and reliability of large-eddy simulations II, Springer, pp 149–160
Catalano F, Cenedese A (2010) High-resolution numerical modeling of thermally driven slope winds in a valley with strong capping. J Appl Meteorol Climatol 49(9):1859–1880
Charrondière C, Brun C, Sicart JE, Cohard JM, Biron R, Blein S (2020) Buoyancy effects in the turbulence kinetic energy budget and reynolds stress budget for a katabatic jet over a steep alpine slope. Boundary-Layer Meteorol 177(1):97–122
Charrondiére C, Brun C, Hopfinger EJ, Cohard JM, Sicart J (2022) Mean flow structure of katabatic winds and turbulent mixing properties. J Fluid Mechan 941:A11. Cambridge University Press
Charrondière C, Brun C, Cohard JM, Sicart JE, Obligado M, Biron R, Coulaud C, Guyard H (2022) Katabatic winds over steep slopes: overview of a field experiment designed to investigate slope-normal velocity and near-surface turbulence. Boundary-Layer Meteorol 182:29–54
Chemel C, Staquet C, Largeron Y (2009) Generation of internal gravity waves by a katabatic wind in an idealized alpine valley. Meteorol Atmos Phys 103(1):187–194
Chen H, Yi C (2012) Optimal control of katabatic flows within canopies. Q J R Meteorol Soc 138(667):1676–1680
Chow FK, Schär C, Ban N, Lundquist KA, Schlemmer L, Shi X (2019) Crossing multiple gray zones in the transition from mesoscale to microscale simulation over complex terrain. Atmosphere 10(5):274
Cintolesi C, Di Santo D, Barbano F, Di Sabatino S (2021) Anabatic flow along a uniformly heated slope studied through Large-Eddy Simulation. Atmosphere 12(7):850
Cuxart J, Morales G, Terradellas E, Yagüe C (2002) Study of coherent structures and estimation of the pressure transport terms for the nocturnal stable boundary layer. Boundary-Layer Meteorol 105(2):305–328
Cuxart J, Martínez-Villagrasa D, Stiperski I (2020) Validation of a simple diagnostic relationship for downslope flows. Atmos Sci Lett 21(5):965
Darby LS, Allwine KJ, Banta RM (2006) Nocturnal low-level jet in a mountain basin complex. Part II: Transport and diffusion of tracer under stable conditions. J Appl Meteorol Climatol 45(5):740–753
De Wekker S, Steyn D, Nyeki S (2004) A comparison of aerosol-layer and convective boundary-layer structure over a mountain range during STAAARTE'97. Boundary-Layer Meteorol 113(2):249–271
De Wekker SF, Kossmann M (2015) Convective boundary layer heights over mountainous terrain–a review of concepts. Front Earth Sci 3:77
De Wekker SF, Kossmann M, Knievel JC, Giovannini L, Gutmann ED, Zardi D (2018) Meteorological applications benefiting from an improved understanding of atmospheric exchange processes over mountains. Atmosphere 9(10):371
Defant F (1949) Zur theorie der hangwinde, nebst bemerkungen zur theorie der berg-und talwinde. Archiv für Meteorologie, Geophysik und Bioklimatologie, Serie A 1(3):421–450
Demko JC (2009) An observational and numerical modeling study of the evolving convective boundary layer and orographic circulation around the Santa Catalina Mountains in Arizona
Denby B, Smeets C (2000) Derivation of turbulent flux profiles and roughness lengths from katabatic flow dynamics. J Appl Meteorol Climatol 39(9):1601–1612
Drake S, Higgins C, Pardyjak E (2021) Distinguishing time scales of katabatic flow in complex terrain. Atmosphere 12(12):1651
Drake SA, Rupp DE, Thomas CK, Oldroyd HJ, Schulze M, Jones JA (2022) Increasing daytime stability enhances downslope moisture transport in the subcanopy of an even-aged conifer forest in western Oregon, USA. J Geophys Res Atmos 127(9):1
Ebner L, Heinemann G, Haid V, Timmermann R (2014) Katabatic winds and polynya dynamics at Coats Land. Antarctica. Antarctic Sci 26(3):309–326

Emeis S, Kalthoff N, Adler B, Pardyjak E, Paci A, Junkermann W (2018) High-resolution observations of transport and exchange processes in mountainous terrain. Atmosphere 9(12):457
Everard KA, Oldroyd HJ, Christen A (2020) Turbulent heat and momentum exchange in nocturnal drainage flow through a sloped vineyard. Boundary-Layer Meteorol 175(1):1–23
Farina S, Marchio M, Barbano F, Di Sabatino S, Zardi D (2023) Characterization of the morning transition over the gentle slope of a semi-isolated massif. J Appl Meteorol Climatol 62(4):449–466
Fedorovich E, Shapiro A (2009) Structure of numerically simulated katabatic and anabatic flows along steep slopes. Acta Geophys 57(4):981–1010
Fedorovich E, Gibbs JA, Shapiro A (2017) Numerical study of nocturnal low-level jets over gently sloping terrain. J Atmos Sci 74(9):2813–2834
Feigenwinter C, Bernhofer C, Eichelmann U, Heinesch B, Hertel M, Janous D, Kolle O, Lagergren F, Lindroth A, Minerbi S et al (2008) Comparison of horizontal and vertical advective CO2 fluxes at three forest sites. Agric For Meteorol 148(1):12–24
Fernando H, Pardyjak E, Di Sabatino S, Chow F, De Wekker S, Hoch S, Hacker J, Pace J, Pratt T, Pu Z et al (2015) The MATERHORN: unraveling the intricacies of mountain weather. Bull Am Meteor Soc 96(11):1945–1967
Fernando HJ, Verhoef B, Di Sabatino S, Leo LS, Park S (2013) The phoenix evening transition flow experiment (TRANSFLEX). Boundary-Layer Meteorol 147(3):443–468
Fernando HJS, Mann J, Palma JMLM, Lundquist JK, Barthelmie RJ, Belo-Pereira M, Brown WOJ, Chow FK, Gerz T, Hocut CM, Klein PM, Leo LS, Matos JC, Oncley SP, Pryor SC, Bariteau L, Bell TM, Bodini N, Carney MB, Courtney MS, Creegan ED, Dimitrova R, Gomes S, Hagen M, Hyde JO, Kigle S, Krishnamurthy R, Lopes JC, Mazzaro L, Neher JMT, Menke R, Murphy P, Oswald L, Otarola-Bustos S, Pattantyus AK, Rodrigues CV, Schady A, Sirin N, Spuler S, Svensson E, Tomaszewski J, Turner DD, van Veen L, Vasiljević N, Vassallo D, Voss S, Wildmann N, Wang Y (2019) The perdigão: Peering into microscale details of mountain winds. Bull Am Meteor Soc 100(5):799–819
Finnigan J, Ayotte K, Harman I, Katul G, Oldroyd H, Patton E, Poggi D, Ross A, Taylor P (2020) Boundary-layer flow over complex topography. Boundary-Layer Meteorol 177(2):247–313
Fleagle RG (1950) A theory of air drainage. J Atmos Sci 7(3):227–232
Geerts B, Miao Q, Demko JC (2008) Pressure perturbations and upslope flow over a heated, isolated mountain. Mon Weather Rev 136(11):4272–4288
Georg W, Albin H, Georg N, Katharina S, Enrico T, Peng Z (2016) On the energy balance closure and net radiation in complex terrain. Agric For Meteorol 226:37–49
Giometto M, Katul G, Fang J, Parlange M (2017) Direct numerical simulation of turbulent slope flows up to Grashof number. J Fluid Mech 829:589–620
Giovannini L, Laiti L, Serafin S, Zardi D (2017) The thermally driven diurnal wind system of the Adige Valley in the Italian Alps. Q J R Meteorol Soc 143(707):2389–2402
Gohm A, Harnisch F, Vergeiner J, Obleitner F, Schnitzhofer R, Hansel A, Fix A, Neininger B, Emeis S, Schaefer K (2009) Air pollution transport in an Alpine valley: Results from airborne and ground-based observations. Boundary-Layer Meteorol 131:441–463
Grachev AA, Leo LS, Di Sabatino S, Fernando HJ, Pardyjak ER, Fairall CW (2016) Structure of turbulence in katabatic flows below and above the wind-speed maximum. Boundary-Layer Meteorol 159(3):469–494
Grazioli J, Madeleine JB, Gallée H, Forbes RM, Genthon C, Krinner G, Berne A (2017) Katabatic winds diminish precipitation contribution to the Antarctic ice mass balance. Proc Natl Acad Sci 114(41):10,858-10,863
Grisogono B, Axelsen SL (2012) A note on the pure katabatic wind maximum over gentle slopes. Boundary-Layer Meteorol 145(3):527–538
Grisogono B, Oerlemans J (2001) A theory for the estimation of surface fluxes in simple katabatic flows. Q J R Meteorol Soc 127(578):2725–2739
Grisogono B, Oerlemans J (2002) Justifying the WKB approximation in pure katabatic flows. Tellus A: Dyn Meteorol Oceanogr 54(5):453–462
Grisogono B, Kraljević L, Jeričević A (2007) The low-level katabatic jet height versus Monin-Obukhov height. Q J R Meteorol Soc 133(629):2133–2136
Grisogono B, Jurlina T, Večenaj Ž, Güttler I (2015) Weakly nonlinear Prandtl model for simple slope flows. Q J R Meteorol Soc 141(688):883–892
Güttler I, Marinović I, Večenaj Ž, Grisogono B (2016) Energetics of slope flows: linear and weakly nonlinear solutions of the extended Prandtl model. Front Earth Sci 4:72
Güttler I, Marinović I, Večenaj Ž, Grisogono B (2017) Corrigendum: energetics of slope flows: Linear and weakly nonlinear solutions of the extended Prandtl model. Front Earth Sci 5:76
Haiden T (2003) On the pressure field in the slope wind layer. J Atmos Sci 60(13):1632–1635

Haiden T, Whiteman CD (2005) Katabatic flow mechanisms on a low-angle slope. J Appl Meteorol 44(1):113–126

Hammerle A, Haslwanter A, Schmitt M, Bahn M, Tappeiner U, Cernusca A, Wohlfahrt G (2007) Eddy covariance measurements of carbon dioxide, latent and sensible energy fluxes above a meadow on a mountain slope. Boundary-Layer Meteorol 122:397–416

Hang C, Nadeau DF, Jensen DD, Hoch SW, Pardyjak ER (2016) Playa soil moisture and evaporation dynamics during the materhorn field program. Boundary-Layer Meteorol 159(3):521–538

Hang C, Oldroyd HJ, Giometto MG, Pardyjak ER, Parlange MB (2021) A local similarity function for katabatic flows derived from field observations over steep- and shallow-angled slopes. Geophys Res Lett 48(23):e2021GL095,479. https://doi.org/10.1029/2021GL095479

Hang C, Oldroyd HJ, Giometto MG, Pardyjak ER, Parlange MB (2021) A local similarity function for katabatic flows derived from field observations over steep-and shallow-angled slopes. Geophys Res Lett 48(23):e2021GL095,479

Harnisch F, Gohm A, Fix A, Schnitzhofer R, Hansel A, Neininger B (2009) Spatial distribution of aerosols in the Inn Valley atmosphere during wintertime. Meteorol Atmos Phys 103:223–235

Heinemann G (2002) Aircraft-based measurements of turbulence structures in the katabatic flow over Greenland. Boundary-Layer Meteorol 103(1):49–81

Heinemann G (2004) Local similarity properties of the continuously turbulent stable boundary layer over Greenland. Boundary-Layer Meteorol 112(2):283–305

Heinesch B, Yernaux Y, Aubinet M (2008) Dependence of CO2 advection patterns on wind direction on a gentle forested slope. Biogeosciences 5(3):657–668

Henao-Garcia S, Xiao CN, Senocak I (2022) Investigation of oscillations in katabatic Prandtl slope flows. Q J R Meteorol Soc

Hewitt RUJ, A W, (2023) Shallow katabatic flow on a non-uniformly cooled slope. Environ Fluid Mech 23:351–368. https://doi.org/10.1007/s10652-022-09887-w

Hilel Goldshmid R, Liberzon D (2020) Obtaining turbulence statistics of thermally driven anabatic flow by sonic-hot-film combo anemometer. Environ Fluid Mech 20(5):1221–1249

Hilel Goldshmid R, Bardoel SL, Hocut CM, Zhong Q, Liberzon D, Fernando HJ (2018) Separation of upslope flow over a plateau. Atmosphere 9(5):165

Hiller R, Zeeman MJ, Eugster W (2008) Eddy-covariance flux measurements in the complex terrain of an Alpine valley in Switzerland. Boundary-Layer Meteorol 127:449–467

Hoch SW, Whiteman CD (2010) Topographic effects on the surface radiation balance in and around Arizona's Meteor Crater. J Appl Meteorol Climatol 49(6):1114–1128

Hocut C, Liberzon D, Fernando H (2015) Separation of upslope flow over a uniform slope. J Fluid Mech 775:266–287

Hunt J, Fernando H, Princevac M (2003) Unsteady thermally driven flows on gentle slopes. J Atmos Sci 60(17):2169–2182

Ingel'L K (2000) Nonlinear theory of slope flows. Izv Atmos Ocean Phys 36(3):384–389

Jensen DD, Nadeau DF, Hoch SW, Pardyjak ER (2017) The evolution and sensitivity of katabatic flow dynamics to external influences through the evening transition. Q J R Meteorol Soc 143(702):423–438

Jiang Q, Doyle JD (2008) Diurnal variation of downslope winds in Owens Valley during the Sierra Rotor Experiment. Mon Weather Rev 136(10):3760–3780

Kirshbaum DJ (2013) On thermally forced circulations over heated terrain. J Atmos Sci 70:1690–1709. https://doi.org/10.1175/JAS-D-12-0199.1

Klein T, Heinemann G, Bromwich DH, Cassano JJ, Hines KM (2001) Mesoscale modeling of katabatic winds over greenland and comparisons with AWS and aircraft data. Meteorol Atmos Phys 78(1):115–132

Kossmann M, Fiedler F (2000) Diurnal momentum budget analysis of thermally induced slope winds. Meteorol Atmos Phys 75:195–215. https://doi.org/10.1007/s007030070004

Largeron Y, Staquet C, Chemel C (2010) Turbulent mixing in a katabatic wind under stable conditions. Meteorologische Zeitschrift 467–480

Lehner M, Gohm A (2010) Idealised simulations of daytime pollution transport in a steep valley and its sensitivity to thermal stratification and surface albedo. Boundary-Layer Meteorol 134(2):327–351

Lehner M, Whiteman CD, Hoch SW, Jensen D, Pardyjak ER, Leo LS, Di Sabatino S, Fernando HJ (2015) A case study of the nocturnal boundary layer evolution on a slope at the foot of a desert mountain. J Appl Meteorol Climatol 54(4):732–751

Lehner M, Rotunno R, Whiteman CD (2016) Flow regimes over a basin induced by upstream katabatic flows–an idealized modeling study. J Atmos Sci 73(10):3821–3842

Lehner M, Rotach MW, Obleitner F (2019) A method to identify synoptically undisturbed, clear-sky conditions for valley-wind analysis. Boundary-Layer Meteorol 173(3):435–450

Lin YT, Wu CH (2015) Effects of a sharp change of emergent vegetation distributions on thermally driven flow over a slope. Environ Fluid Mech 15(4):771–791
Lin-Lin W, Xiao-Feng G, Bing-Cheng W (2014) Characteristics of thermally-induced near-surface flows over an enclosed crater: observations of the meteor crater experiment (metcrax). Atmos Ocean Sci Lett 7(2):162–167
Łobocki L (2014) Surface-layer flux-gradient relationships over inclined terrain derived from a local equilibrium, turbulence closure model. Boundary-Layer Meteorol 150(3):469–483
Łobocki L (2017) Turbulent mechanical energy budget in stably stratified baroclinic flows over sloping terrain. Boundary-Layer Meteorol 164(3):353–365
Lykosov V, Gutman L (1972) Turbulent boundary-layer over a sloping underlying surface. IZVESTIYA1589 Akademii Nauk Sssr Fizika Atmosfery I Okeana 8(8):799
Lothon M, Lohou F, Pino D, Couvreux F, Pardyjak ER, Reuder J,Vilà-Guerau de Arellano, Jordi and Durand, Pierre and Hartogensis O, Legain, Dominique (2014) The BLLAST field experiment: boundary-layer late afternoon and sunset turbulence. Atmos Chem Phy 14 (20):10931–10960
Mahrt L, Richardson S, Seaman N, Stauffer D (2010) Non-stationary drainage flows and motions in the cold pool. Tellus A: Dyn Meteorol Oceanogr 62(5):698–705
Martínez D, Cuxart J (2009) Assessment of the hydraulic slope flow approach using a mesoscale model. Acta Geophys 57(4):882–903
Massey JD, Steenburgh WJ, Hoch SW, Jensen DD (2017) Simulated and observed surface energy fluxes and resulting playa breezes during the MATERHORN field campaigns. J Appl Meteorol Climatol 56(4):915–935
Matzinger N, Andretta M, Gorsel EV, Vogt R, Ohmura A, Rotach MW (2003) Surface radiation budget in an alpine valley. Q J R Meteorol Soc 129(588):877–895
Mo R (2013) On adding thermodynamic damping mechanisms to refine two classical models of katabatic winds. J Atmos Sci 70(7):2325–2334
Monti P, Fernando H, Princevac M, Chan W, Kowalewski T, Pardyjak E (2002) Observations of flow and turbulence in the nocturnal boundary layer over a slope. J Atmos Sci 59(17):2513–2534
Monti P, Fernando H, Princevac M (2014) Waves and turbulence in katabatic winds. Environ Fluid Mech 14:431–450
Moroni M, Giorgilli M, Cenedese A (2014) Experimental investigation of slope flows via image analysis techniques. J Atmos Solar Terr Phys 108:17–33
Nadeau DF, Pardyjak ER, Higgins CW, Huwald H, Parlange MB (2013) Flow during the evening transition over steep alpine slopes. Q J R Meteorol Soc 139(672):607–624
Nadeau DF, Oldroyd HJ, Pardyjak ER, Sommer N, Hoch SW, Parlange MB (2020) Field observations of the morning transition over a steep slope in a narrow alpine valley. Environ Fluid Mech 20(5):1199–1220
Nicholson L, Stiperski I (2020) Comparison of turbulent structures and energy fluxes over exposed and debris-covered glacier ice. J Glaciol 66(258):543–555
Noppel H, Fiedler F (2002) Mesoscale heat transport over complex terrain by slope winds–a conceptual model and numerical simulations. Boundary-Layer Meteorol 104(1):73–97
Oerlemans J, Grisogono B (2002) Glacier winds and parameterisation of the related surface heat fluxes. Tellus A: Dyn Meteorol Oceanogr 54(5):440–452
Oldroyd HJ, Pardyjak ER, Huwald H, Parlange MB(2016) Adapting tilt corrections and the governing flow equations for steep, fully three-dimensional, mountainous terrain. Boundary-layer meteorology 159:539–565
Oldroyd HJ, Katul G, Pardyjak ER, Parlange MB (2014) Momentum balance of katabatic flow on steep slopes covered with short vegetation. Geophys Res Lett 41(13):4761–4768
Oldroyd HJ, Pardyjak ER, Higgins CW, Parlange MB (2016) Buoyant turbulent kinetic energy production in steep-slope katabatic flow. Boundary-Layer Meteorol 161(3):405–416
Oltmanns M, Straneo F, Seo H, Moore G (2015) The role of wave dynamics and small-scale topography for downslope wind events in southeast Greenland. J Atmos Sci 72(7):2786–2805
Papadopoulos K, Helmis C (1999) Evening and morning transition of katabatic flows. Boundary-Layer Meteorol 92(2):195–227
Paperman J, Potchter O, Alpert P (2022) Characteristics of the summer 3-d katabatic flow in a semi-arid zone-the case of the Dead Sea. Int J Climatol 42(3):1975–1984
Pardyjak ER, Fernando HJS, Hunt JC, Grachev AA, Anderson J (2009) A case study of the development of nocturnal slope flows in a wide open valley and associated air quality implications. Meteorol Z 18(1):85
Parish TR, Cassano JJ (2003) The role of katabatic winds on the antarctic surface wind regime. Mon Weather Rev 131(2):317–333
Parmhed O, Oerlemans J, Grisogono B (2004) Describing surface fluxes in katabatic flow on Breidamerkurjökull. Iceland. Q J R Meteorol Soc 130(598):1137–1151

Porson A, Steyn DG, Schayes G (2007) Sea-breeze scaling from numerical model simulations, part II: Interaction between the sea breeze and slope flows. Boundary-Layer Meteorol 122(1):31–41
Poulos G, Zhong S (2008) An observational history of small-scale katabatic winds in mid-latitudes. Geogr Compass 2(6):1798–1821
Poulos GS, Bossert JE, McKee TB, Pielke RA (2000) The interaction of katabatic flow and mountain waves. part I: Observations and idealized simulations. J Atmos Sci 57(12):1919–1936
Poulos GS, Bossert JE, McKee TB, Pielke RA (2007) The interaction of katabatic flow and mountain waves. part II: Case study analysis and conceptual model. J Atmos Sci 64(6):1857–1879
Prandtl L (1942) Führer durch die strömungslehre, chapter 5. Friedrich Vieweg & Sohn, pp 326–330
Princevac M, Fernando H (2007) A criterion for the generation of turbulent anabatic flows. Phys Fluids 19(10):105,102
Princevac M, Hunt J, Fernando H (2008) Quasi-steady katabatic winds on slopes in wide valleys: hydraulic theory and observations. J Atmos Sci 65(2):627–643
Prtenjak MT, Klaić M, Jeričević A, Cuxart J (2018) The interaction of the downslope winds and fog formation over the Zagreb area. Atmos Res 214:213–227
Radić, V., Menounos, B., Shea, J., Fitzpatrick, N., Tessema, M.A., Déry, S.J. (2017) Evaluation of different methods to model near-surface turbulent fluxes for a mountain glacier in the Cariboo Mountains, BC, Canada. The Cryosphere 11(6):2897–2918, Copernicus GmbH
Renfrew IA (2004) The dynamics of idealized katabatic flow over a moderate slope and ice shelf. Q J R Meteorol Soc 130(598):1023–1045
Renfrew IA, Anderson PS (2006) Profiles of katabatic flow in summer and winter over Coats Land. Antarctica. Q J R Meteorol Soc 132(616):779–802
Reuten C, Steyn D, Strawbridge K, Bovis P (2005) Observations of the relation between upslope flows and the convective boundary layer in steep terrain. Boundary-Layer Meteorol 116(1):37–61
Reuten C, Steyn D, Allen S (2007) Water tank studies of atmospheric boundary layer structure and air pollution transport in upslope flow systems. J Geophys Res: Atmos 112(D11)
Román-Cascón C, Yagüe C, Arrillaga J, Lothon M, Pardyjak E, Lohou F, Inclán R, Sastre M, Maqueda G, Derrien S et al (2019) Comparing mountain breezes and their impacts on CO2 mixing ratios at three contrasting areas. Atmos Res 221:111–126
Rotach MW, Serafin S, Ward HC, Arpagaus M, Colfescu I, Cuxart J, De Wekker, Stephan FJ (2022) A collaborative effort to better understand, measure, and model atmospheric exchange processes over mountains. Bull Am Meteor Soci 103 (5):E1282–E1295
Rotach MW, Calanca P, Graziani G, Gurtz J, Steyn DG, Vogt R, Andretta M, Christen A, Cieslik S, Connolly R et al (2004) Turbulence structure and exchange processes in an Alpine valley: The Riviera project. Bull Am Meteor Soc 85(9):1367–1386
Rotach MW, Andretta M, Calanca P, Weigel AP, Weiss A (2008) Boundary layer characteristics and turbulent exchange mechanisms in highly complex terrain. Acta Geophys 56(1):194–219
Rotach MW, Stiperski I, Fuhrer O, Goger B, Gohm A, Obleitner F, Rau G, Sfyri E, Vergeiner J (2017) Investigating exchange processes over complex topography: The Innsbruck box (i-Box). Bull Am Meteor Soc 98(4):787–805
Sastre M, Yagüe C, Román-Cascón C, Maqueda G (2015) Atmospheric boundary-layer evening transitions: a comparison between two different experimental sites. Boundary-Layer Meteorol 157(3):375–399
Savage III LC, Zhong S, Yao W, Brown WJ, Horst TW, Whiteman CD (2008) An observational and numerical study of a regional-scale downslope flow in northern Arizona. Journal of Geophysical Research: Atmospheres 113(D14)
Schmidli J (2013) Daytime heat transfer processes over mountainous terrain. J Atmos Sci 70(12):4041–4066
Schumann U (1990) Large-eddy simulation of the up-slope boundary layer. Q J R Meteorol Soc 116:637–670
Senocak I, Xiao CN (2020) Linear Instability of Stably Stratified Down-Slope Flows. Springer, Singapore, pp 47–68
Seo JM, Ganbat G, Han JY, Baik JJ (2017) Theoretical calculations of interactions between urban breezes and mountain slope winds in the presence of basic-state wind. Theoret Appl Climatol 127(3–4):865–874
Serafin S, Zardi D (2010) Daytime heat transfer processes related to slope flows and turbulent convection in an idealized mountain valley. J Atmos Sci 67(11):3739–3756. https://doi.org/10.1175/2010JAS3428.1
Serafin S, Zardi D (2010) Structure of the atmospheric boundary layer in the vicinity of a developing upslope flow system: a numerical model study. J Atmos Sci 67(4):1171–1185
Serafin S, Zardi D (2011) Daytime development of the boundary layer over a plain and in a valley under fair weather conditions: a comparison by means of idealized numerical simulations. J Atmos Sci 68(9):2128–2141. https://doi.org/10.1175/2011JAS3610.1

Serafin S, Adler B, Cuxart J, De Wekker SF, Gohm A, Grisogono B, Kalthoff N, Kirshbaum DJ, Rotach MW, Schmidli J et al (2018) Exchange processes in the atmospheric boundary layer over mountainous terrain. Atmosphere 9(3):102

Serafin S, Rotach MW, Arpagaus M, Colfescu I, Cuxart J, De Wekker SFJ, Evans M, Grubišić V, Kalthoff N, Karl T, Kirshbaum DJ, Lehner M, Mobbs S, Paci A, Palazzi E, Bailey A, Schmidli J, Wohlfahrt G, Zardi D. (2020) Multi-scale transport and exchange processes in the atmosphere over mountains. Innsbruck University Press, p 42

Serrano-Ortiz P, Sánchez-Cañete E, Olmo F, Metzger S, Pérez-Priego O, Carrara A, Alados-Arboledas L, Kowalski A (2016) Surface-parallel sensor orientation for assessing energy balance components on mountain slopes. Boundary-Layer Meteorol 158:489–499

Sfyri E, Rotach MW, Stiperski I, Bosveld FC, Lehner M, Obleitner F (2018) Scalar-flux similarity in the layer near the surface over mountainous terrain. Boundary-Layer Meteorol 169(1):11–46

Shapiro A, Fedorovich E (2007) Katabatic flow along a differentially cooled sloping surface. J Fluid Mech 571:149–175

Shapiro A, Fedorovich E (2014) A boundary-layer scaling for turbulent katabatic flow. Boundary-Layer Meteorol 153(1):1–17

Shapiro A, Burkholder B, Fedorovich E (2012) Analytical and numerical investigation of two-dimensional katabatic flow resulting from local surface cooling. Boundary-Layer Meteorol 145(1):249–272

Shindler L, Giorgilli M, Moroni M, Cenedese A (2013) Investigation of local winds in a closed valley: an experimental insight using Lagrangian particle tracking. J Wind Eng Ind Aerodyn 114:1–11

Skyllingstad ED (2003) Large-eddy simulation of katabatic flows. Boundary-Layer Meteorol 106(2):217–243

Smith CM, Porté-Agel F (2014) An intercomparison of subgrid models for large-eddy simulation of katabatic flows. Q J R Meteorol Soc 140(681):1294–1303

Smith CM, Skyllingstad ED (2005) Numerical simulation of katabatic flow with changing slope angle. Mon Weather Rev 133(11):3065–3080

Söderberg S, Parmhed O (2006) Numerical modelling of katabatic flow over a melting outflow glacier. Boundary-Layer Meteorol 120(3):509–534

Spall MA, Jackson RH, Straneo F (2017) Katabatic wind-driven exchange in fjords. J Geophys Res: Oceans 122(10):8246–8262

Spoeck G, Arbeiter M (2021) Determining slope-and free air flow wind profiles for WKB Prandtl models

Stiperski I, Kavčič I, Grisogono B, Durran DR (2007) Including Coriolis effects in the Prandtl model for katabatic flow. Q J R Meteorol Soc: J Atmos Sci Appl Meteorol Physical Oceanogr 133(622):101–106

Stiperski I, Holtslag AA, Lehner M, Hoch SW, Whiteman CD (2020) On the turbulence structure of deep katabatic flows on a gentle mesoscale slope. Q J R Meteorol Soc 146(728):1206–1231

Trachte K, Bendix J (2012) Katabatic flows and their relation to the formation of convective clouds-idealized case studies. J Appl Meteorol Climatol 51(8):1531–1546

Trachte K, Nauss T, Bendix J (2010) The impact of different terrain configurations on the formation and dynamics of katabatic flows: idealised case studies. Boundary-Layer Meteorol 134(2):307–325

Umphrey C, DeLeon R, Senocak I (2017) Direct numerical simulation of turbulent katabatic slope flows with an immersed-boundary method. Boundary-Layer Meteorol 164(3):367–382

Van Der Avoird E, Duynkerke PG (1999) Turbulence in a katabatic flow. Boundary-Layer Meteorol 92(1):37–63

Van Gorsel E, Christen A, Feigenwinter C, Parlow E, Vogt R (2003) Daytime turbulence statistics above a steep forested slope. Boundary-Layer Meteorol 109(3):311–329

Villagrasa DM, Lehner M, Whiteman CD, Hoch SW, Cuxart J (2013) The upslope-downslope flow transition on a basin sidewall. J Appl Meteorol Climatol 52(12):2715–2734

Wang X, Wang C, Li Q (2015) Wind regimes above and below a temperate deciduous forest canopy in complex terrain: interactions between slope and valley winds. Atmosphere 6(1):60–87

Weigel AP, Rotach MW (2004) Flow structure and turbulence characteristics of the daytime atmosphere in a steep and narrow Alpine valley. Q J R Meteorol Soc: J Atmos Sci Appl Meteorol Phys Oceanogr 130(602):2605–2627

Whiteman CD (2000) Mountain meteorology: fundamentals and applications. Oxford University Press, Oxford

Whiteman CD, Zhong S (2008) Downslope flows on a low-angle slope and their interactions with valley inversions. Part I: Observations. J Appl Meteorol Climatol 47(7):2023–2038

Whiteman CD, Eisenbach S, Pospichal B, Steinacker R (2004) Comparison of vertical soundings and sidewall air temperature measurements in a small alpine basin. J Appl Meteorol 43(11):1635–1647

Whiteman CD, Muschinski A, Zhong S, Fritts D, Hoch SW, Hahnenberger M, Yao W, Hohreiter V, Behn M, Cheon Y et al (2008) METCRAX 2006: meteorological experiments in Arizona's meteor crater. Bull Am Meteor Soc 89(11):1665–1680

Xiao CN, Senocak I (2019) Stability of the Prandtl model for katabatic slope flows. J. Fluid Mech.865

Xiao CN, Senocak I (2020a) Linear stability of katabatic prandtl slope flows with ambient wind forcing. J Fluid Mech 886:R1
Xiao CN, Senocak I (2020b) Stability of the anabatic Prandtl slope flow in a stably stratified medium. J Fluid Mech 885
Xiao CN, Senocak I (2022) Speaker-wire vortices in stratified anabatic prandtl slope flows and their secondary instabilities. J Fluid Mech 944:A27
Yi C, Monson RK, Zhai Z, Anderson DE, Lamb B, Allwine G, Turnipseed AA, Burns SP (2005) Modeling and measuring the nocturnal drainage flow in a high-elevation, subalpine forest with complex terrain. J Geophys Res: Atmospheres 110(D22)
Zakarin E, Baklanov A, Balakay L, Dedova T, Bostanbekov K (2022) Modeling of the calm situations in the atmosphere of almaty. Asian J Atmos Environ 16(2):2022,007
Zardi D, Serafin S (2015) An analytic solution for time-periodic thermally driven slope flows. Q J R Meteorol Soc 141(690):1968–1974
Zardi D, Whiteman CD (2013) Diurnal mountain wind systems. Mountain weather research and forecasting: Recent progress and current challenges, pp 35–119
Zhong S, Whiteman CD (2008) Downslope flows on a low-angle slope and their interactions with valley inversions. Part II: Numerical modeling. J Appl Meteorol Climatol 47(7):2039–2057
Zilitinkevich SS, Hunt JCR, Esau IN, Grachev AA, Lalas DP, AKYLAS E, Tombrou M, Fairall CW, Fernando HJS, Baklanov AA, Joffre SM, (2006) The influence of large convective eddies on the surface-layer turbulence. Q J R Meteorol Soc 132(618):1426–1456
Zilitinkevich SS, Elperin T, Kleeorin N, Rogachevskii I (2007) Energy- and flux-budget (efb) turbulence closure model for stably stratified flows. Part i: steady-state, homogeneous regimes. Boundary-Layer Meteorol 125(2):167–191
Zilitinkevich SS, Elperin T, Kleeorin N, Rogachevskii I, Esau I, Mauritsen T, Miles MW (2008) Turbulence energetics in stably stratified geophysical flows: Strong and weak mixing regimes. Q J R Meteorol Soc 134(633):793–799
Zwinger T, Malm T, Schäfer M, Stenberg R, Moore J (2015) Interaction of katabatic wind and local surface mass balance at Scharffenbergbotnen Blue Ice Area. Antarctica. Cryosphere Discuss 9(2):1